10. Electroweak Model and Constraints on New Physics

Revised March 2018 by J. Erler (U. Mexico) and A. Freitas (Pittsburgh U.).

10.1. Introduction

The standard model of the electroweak interactions (SM) [1] is based on the gauge group SU(2) × U(1), with gauge bosons W^i_μ, $i = 1, 2, 3$, and B_μ for the SU(2) and U(1) factors, respectively, and the corresponding gauge coupling constants g and g'. The left-handed fermion fields of the $i^{\rm th}$ fermion family transform as doublets $\Psi_i = \begin{pmatrix} \nu_i \\ \ell_i^- \end{pmatrix}$ and $\begin{pmatrix} u_i \\ d'_i \end{pmatrix}$ under SU(2), where $d'_i \equiv \sum_j V_{ij}\, d_j$, and V is the Cabibbo-Kobayashi-Maskawa mixing matrix. [Constraints on V and tests of universality are discussed in Ref. 2 and in the Section on "The CKM Quark-Mixing Matrix". The extension of the formalism to allow an analogous leptonic mixing matrix is discussed in the Section on "Neutrino Mass, Mixing, and Oscillations".] The right-handed fields are SU(2) singlets. From Higgs and electroweak precision data it is known that there are precisely three sequential fermion families.

A complex scalar Higgs doublet, $\phi \equiv \begin{pmatrix} \phi^+ \\ \phi^0 \end{pmatrix}$, is added to the model for mass generation through spontaneous symmetry breaking with potential* given by,

$$V(\phi) = \mu^2 \phi^\dagger \phi + \frac{\lambda^2}{2} (\phi^\dagger \phi)^2. \tag{10.1}$$

For μ^2 negative, ϕ develops a vacuum expectation value, $v/\sqrt{2} = \mu/\lambda$, where $v \approx 246$ GeV, breaking part of the electroweak (EW) gauge symmetry, after which only one neutral Higgs scalar, H, remains in the physical particle spectrum. In non-minimal models there are additional charged and neutral scalar Higgs particles [3].

After symmetry breaking the Lagrangian for the fermion fields, ψ_i, is

$$\mathscr{L}_F = \sum_i \overline{\psi}_i \left(i \not{\partial} - m_i - \frac{m_i H}{v} \right) \psi_i$$

* There is no generally accepted convention to write the quartic term. Our numerical coefficient simplifies Eq. (10.3a) below and the squared coupling preserves the relation between the number of external legs and the power counting of couplings at a given loop order. This structure also naturally emerges from physics beyond the SM, such as supersymmetry.

$$
\begin{aligned}
&- \frac{g}{2\sqrt{2}} \sum_i \overline{\Psi}_i \, \gamma^\mu \, (1-\gamma^5)(T^+ \, W_\mu^+ + T^- \, W_\mu^-) \, \Psi_i \\
&- e \sum_i Q_i \, \overline{\psi}_i \, \gamma^\mu \, \psi_i \, A_\mu \\
&- \frac{g}{2\cos\theta_W} \sum_i \overline{\psi}_i \, \gamma^\mu (g_V^i - g_A^i \gamma^5) \, \psi_i \, Z_\mu \ . \qquad (10.2)
\end{aligned}
$$

Here $\theta_W \equiv \tan^{-1}(g'/g)$ is the weak angle; $e = g \sin\theta_W$ is the positron electric charge; and $A \equiv B\cos\theta_W + W^3 \sin\theta_W$ is the photon field (γ). $W^\pm \equiv (W^1 \mp iW^2)/\sqrt{2}$ and $Z \equiv -B\sin\theta_W + W^3\cos\theta_W$ are the charged and neutral weak boson fields, respectively. The Yukawa coupling of H to ψ_i in the first term in $\mathscr{L}_F$, which is flavor diagonal in the minimal model, is $gm_i/2M_W$. The boson masses in the EW sector are given (at tree level, *i.e.*, to lowest order in perturbation theory) by,

$$M_H = \lambda \, v, \qquad (10.3a)$$

$$M_W = \frac{1}{2} \, g \, v = \frac{e \, v}{2 \sin\theta_W}, \qquad (10.3b)$$

$$M_Z = \frac{1}{2} \sqrt{g^2 + g'^2} \, v = \frac{e \, v}{2 \sin\theta_W \cos\theta_W} = \frac{M_W}{\cos\theta_W}, \qquad (10.3c)$$

$$M_\gamma = 0. \qquad (10.3d)$$

The second term in $\mathscr{L}_F$ represents the charged-current weak interaction [4–7], where T^+ and T^- are the weak isospin raising and lowering operators. For example, the coupling of a W to an electron and a neutrino is

$$-\frac{e}{2\sqrt{2}\sin\theta_W} \left[W_\mu^- \, \overline{e} \, \gamma^\mu (1-\gamma^5) \nu + W_\mu^+ \, \overline{\nu} \, \gamma^\mu \, (1-\gamma^5) e \right]. \qquad (10.4)$$

For momenta small compared to M_W, this term gives rise to the effective four-fermion interaction with the Fermi constant given by $G_F/\sqrt{2} = 1/2v^2 = g^2/8M_W^2$. CP violation is incorporated into the EW model by a single observable phase in V_{ij}.

The third term in $\mathscr{L}_F$ describes electromagnetic interactions (QED) [8,9], and the last is the weak neutral-current interaction [5–7]. The vector and axial-vector couplings are

$$g_V^i \equiv t_{3L}(i) - 2Q_i \sin^2\theta_W, \qquad (10.5a)$$

$$g_A^i \equiv t_{3L}(i), \qquad (10.5b)$$

where $t_{3L}(i)$ is the weak isospin of fermion i ($+1/2$ for u_i and ν_i; $-1/2$ for d_i and e_i) and Q_i is the charge of ψ_i in units of e.

The first term in Eq. (10.2) also gives rise to fermion masses, and in the presence of right-handed neutrinos to Dirac neutrino masses. The possibility of Majorana masses is discussed in the Section on "Neutrino Mass, Mixing, and Oscillations".

10.2. Renormalization and radiative corrections

In addition to the Higgs boson mass, M_H, the fermion masses and mixings, and the strong coupling constant, α_s, the SM has three parameters. The set with the smallest experimental errors contains the Z mass**, the Fermi constant, and the fine structure constant, which will be discussed in turn (if not stated otherwise, the numerical values quoted in Sec. 10.2–10.5 correspond to the main fit result in Table 10.6):

The Z boson mass, $M_Z = 91.1876 \pm 0.0021$ GeV, has been determined from the Z lineshape scan at LEP 1 [10]. This value of M_Z corresponds to a definition based on a Breit-Wigner shape with an energy-dependent width (see the Section on "The Z Boson" in the Gauge and Higgs Boson Particle Listings of this *Review*).

The Fermi constant, $G_F = 1.1663787(6) \times 10^{-5}$ GeV^{-2}, is derived from the muon lifetime formula***,

$$\frac{\hbar}{\tau_\mu} = \frac{G_F^2 m_\mu^5}{192\pi^3} F(\rho) \left[1 + H_1(\rho)\frac{\widehat{\alpha}(m_\mu)}{\pi} + H_2(\rho)\frac{\widehat{\alpha}^2(m_\mu)}{\pi^2}\right], \tag{10.6}$$

where $\rho = m_e^2/m_\mu^2$, and where

$$F(\rho) = 1 - 8\rho + 8\rho^3 - \rho^4 - 12\rho^2 \ln\rho = 0.99981295, \tag{10.7a}$$

$$H_1(\rho) = \frac{25}{8} - \frac{\pi^2}{2} - \left(9 + 4\pi^2 + 12\ln\rho\right)\rho + 16\pi^2\rho^{3/2} + \mathcal{O}(\rho^2) = -1.80793, \tag{10.7b}$$

$$H_2(\rho) = \frac{156815}{5184} - \frac{518}{81}\pi^2 - \frac{895}{36}\zeta(3) + \frac{67}{720}\pi^4 + \frac{53}{6}\pi^2\ln 2 - (0.042 \pm 0.002)_{\rm had} - \frac{5}{4}\pi^2\sqrt{\rho} + \mathcal{O}(\rho) = 6.64, \tag{10.7c}$$

$$\widehat{\alpha}(m_\mu)^{-1} = \alpha^{-1} + \frac{1}{3\pi}\ln\rho + \mathcal{O}(\alpha) = 135.901 \tag{10.7d}$$

H_1 and H_2 capture the QED corrections within the Fermi model. The results for $\rho = 0$ have been obtained in Refs. 12 and 13, respectively, where the term in parentheses is from the hadronic vacuum polarization [13]. The mass corrections to H_1 have been known for some time [14], while those to H_2 are more recent [15]. Notice the term

** We emphasize that in the fits described in Sec. 10.6 and Sec. 10.7 the values of the SM parameters are affected by all observables that depend on them. This is of no practical consequence for α and G_F, however, since they are very precisely known.

*** In the spirit of the Fermi theory, we incorporated the small propagator correction, $3/5\ m_\mu^2/M_W^2$, into Δr (see below). This is also the convention adopted by the MuLan collaboration [11]. While this breaks with historical consistency, the numerical difference was negligible in the past.

linear in m_e whose appearance was unforeseen and can be traced to the use of the muon pole mass in the prefactor [15]. The remaining uncertainty in G_F is experimental and has been reduced by an order of magnitude by the MuLan collaboration [11] at the PSI. The experimental determination of the fine structure constant, $\alpha = 1/137.035999139(31)$, is currently dominated by the $e^{\pm}$ anomalous magnetic moment [16]. In most EW renormalization schemes, it is convenient to define a running α dependent on the energy scale of the process, with $\alpha^{-1} \sim 137$ appropriate at very low energy, *i.e.* close to the Thomson limit. (The running has also been observed [17] directly.) For scales above a few hundred MeV this introduces an uncertainty due to the low energy hadronic contribution to vacuum polarization. In the modified minimal subtraction ($\overline{\rm MS}$) scheme [18] (used for this *Review*), and with $\alpha_s(M_Z) = 0.1187 \pm 0.0016$ we have $\widehat{\alpha}^{(4)}(m_\tau)^{-1} = 133.476 \pm 0.007$ and $\widehat{\alpha}^{(5)}(M_Z)^{-1} = 127.955 \pm 0.010$. (In this Section we denote quantities defined in the modified minimal subtraction ($\overline{\rm MS}$) scheme by a caret; the exception is the strong coupling constant, α_s, which will always correspond to the $\overline{\rm MS}$ definition and where the caret will be dropped.) The latter corresponds to a quark sector contribution (without the top) to the conventional (on-shell) QED coupling, $\alpha(M_Z) = \dfrac{\alpha}{1 - \Delta\alpha(M_Z)}$, of $\Delta\alpha^{(5)}_{\rm had}(M_Z) = 0.02764 \pm 0.00007$. These values are updated from Ref. 19 with $\Delta\alpha^{(5)}_{\rm had}(M_Z)$ moved downwards and its uncertainty reduced (partly due to a more precise charm quark mass). Its correlation with the $\mu^{\pm}$ anomalous magnetic moment (see Sec. 10.5), as well as the non-linear α_s dependence of $\widehat{\alpha}(M_Z)$ and the resulting correlation with the input variable α_s, are fully taken into account in the fits. This is done by using as actual input (fit constraint) instead of $\Delta\alpha^{(5)}_{\rm had}(M_Z)$ the low energy contribution by the three light quarks, $\Delta\alpha^{(3)}_{\rm had}(2.0\ \text{GeV}) = (58.71 \pm 0.50) \times 10^{-4}$ [20], and by calculating the perturbative and heavy quark contributions to $\widehat{\alpha}(M_Z)$ in each call of the fits according to Ref. 19. Part of the uncertainty ($\pm 0.37 \times 10^{-4}$) is from e^+e^- annihilation data below 1.8 GeV and τ decay data (including uncertainties from isospin breaking effects [21]) , but uncalculated higher order perturbative ($\pm 0.21 \times 10^{-4}$) and non-perturbative ($\pm 0.26 \times 10^{-4}$) [20] QCD corrections and the $\overline{\rm MS}$ quark mass values (see below) also contribute. Various evaluations of $\Delta\alpha^{(5)}_{\rm had}$ are summarized in Table 10.1, where the relation[†] between the $\overline{\rm MS}$ and on-shell definitions (obtained using Ref. 24) is given by

$$\Delta\widehat{\alpha}(M_Z) - \Delta\alpha(M_Z) = \frac{\alpha}{\pi}\left[\frac{100}{27} - \frac{1}{6} - \frac{7}{4}\ln\frac{M_Z^2}{M_W^2} + \frac{\alpha_s(M_Z)}{\pi}\left(\frac{605}{108} - \frac{44}{9}\zeta(3)\right)\right.$$
$$\left. + \frac{\alpha_s^2}{\pi^2}\left(\frac{976481}{23328} - \frac{253}{36}\zeta(2) - \frac{781}{18}\zeta(3) + \frac{275}{27}\zeta(5)\right)\right] = 0.007127(2)\ , \qquad (10.8)$$

[†] In practice, $\alpha(M_Z)$ is directly evaluated in the $\overline{\rm MS}$ scheme using the FORTRAN package GAPP [22], including the QED contributions of both leptons and quarks. The leptonic three-loop contribution in the on-shell scheme has been obtained in Ref. 23.

Table 10.1: Evaluations of the on-shell $\Delta\alpha^{(5)}_{\rm had}(M_Z)$ by different groups (for a more complete list of evaluations see the 2012 edition of this *Review*). For better comparison we adjusted central values and errors to correspond to a common and fixed value of $\alpha_s(M_Z) = 0.120$. References quoting results without the top quark decoupled are converted to the five flavor definition. Ref. [29] uses $\Lambda_{\rm QCD} = 380 \pm 60$ MeV; for the conversion we assumed $\alpha_s(M_Z) = 0.118 \pm 0.003$.

Reference	Result	Comment
Geshkenbein, Morgunov [25]	0.02780 ± 0.00006	$\mathcal{O}(\alpha_s)$ resonance model
Swartz [26]	0.02754 ± 0.00046	use of fitting function
Krasnikov, Rodenberg [27]	0.02737 ± 0.00039	PQCD for $\sqrt{s} > 2.3$ GeV
Kühn & Steinhauser [28]	0.02778 ± 0.00016	full $\mathcal{O}(\alpha_s^2)$ for $\sqrt{s} > 1.8$ GeV
Erler [19]	0.02779 ± 0.00020	conv. from $\overline{\rm MS}$ scheme
Groote *et al.* [29]	0.02787 ± 0.00032	use of QCD sum rules
Martin *et al.* [30]	0.02741 ± 0.00019	incl. new BES data
de Troconiz, Yndurain [31]	0.02754 ± 0.00010	PQCD for $s > 2$ GeV^2
Burkhardt, Pietrzyk [32]	0.02750 ± 0.00033	PQCD for $\sqrt{s} > 12$ GeV
Hagiwara *et al.* [33]	0.02764 ± 0.00014	PQCD: $\sqrt{s} = 2.6{-}3.7, {>}11.1$ GeV
Davier *et al.* [20]	0.02761 ± 0.00008	PQCD: $\sqrt{s} = 1.8{-}3.7, {>}5$ GeV
Jegerlehner [34]	0.02755 ± 0.00011	incl. γ-ρ mixing corrected τ data, Euclidean split technique
Keshavarzi *et al.* [35]	0.02762 ± 0.00011	PQCD for $\sqrt{s} > 11.2$ GeV

and where the first entry of the lowest order term is from fermions and the other two are from $W^\pm$ loops, which are usually excluded from the on-shell definition. Fermion mass effects and corrections of $\mathcal{O}(\alpha\alpha_s^3)$ and $\mathcal{O}(\alpha^2)$ contributing to Eq. (10.8) are small, partly cancel each other and are not included here. The most recent results on $\Delta\alpha^{(5)}_{\rm had}(M_Z)$ [20,34,35] typically assume the validity of perturbative QCD (PQCD) at scales of ~ 2 GeV or above and are in good agreement with each other. In regions where PQCD is not trusted, one can use $e^+e^- \to$ hadrons cross-section data and τ decay spectral functions [36], where the latter derive from OPAL [37], CLEO [38], ALEPH [39], and Belle [40]. Recently, new data for various $e^+e^- \to$ hadrons channels was obtained from Babar, BES3, the SND and CMD3 experiments at VEPP-2M, and the KEDR experiment at VEPP-4M (for a list of references see *e.g.* Ref. 20). While VEPP-2M and VEPP-4M scanned a range of center-of-mass energies in the ranges $\sim$ 1–2 GeV and $\sim$ 3–4 GeV, respectively, the BaBar collaboration studied multi-hadron events radiatively returned from the $\Upsilon(4S)$, reconstructing the radiated photon and

normalizing to $\mu^{\pm}\gamma$ final states. The precision of these results generally exceed those from τ decay spectral functions. There are significant discrepancies between older and newer measurements of $e^+e^- \to K^+K^-$ at SND and CMD, which could be due to difficulties in determining the detection efficiency of low-momentum kaons. The radiative return data from BaBar is expected to be more reliable for this channel owing to an additional boost of the final-state hadrons.

Further free parameters entering into Eq. (10.2) are the quark and lepton masses, where m_i is the mass of the $i^{\rm th}$ fermion ψ_i. For the light quarks, as described in the note on "Quark Masses" in the Quark Listings, $\widehat{m}_u = 2.2^{+0.6}_{-0.4}$ MeV, $\widehat{m}_d = 4.7^{+0.5}_{-0.4}$ MeV, and $\widehat{m}_s = 96^{+8}_{-4}$ MeV. These are running $\overline{\rm MS}$ masses evaluated at the scale $\mu = 2$ GeV. For the charm quark we use the constraint $\widehat{m}_c(\widehat{m}_c) = 1274 \pm 8 + 2616[\alpha_s(M_Z) - 0.1182]$ MeV [41], which is based on QCD sum rules [42,43] and recalculate $\widehat{m}_c$ in each call of our fits to account for its α_s dependence. For the bottom quark we use $\widehat{m}_b(\widehat{m}_b) = 4.180 \pm 0.021$ GeV. To improve the precisions in $\widehat{m}_c(\widehat{m}_c)$ and $\widehat{m}_b(\widehat{m}_b)$ in the future it would help to remeasure the threshold regions of the heavy quarks, as well as the electronic decay widths of the narrow $c\bar{c}$ and $b\bar{b}$ resonances.

The top quark "pole" mass (the quotation marks are a reminder that the experiments do not strictly measure the pole mass and that quarks do not form asymptotic states), has been kinematically reconstructed by the Tevatron Collaborations, CDF and DØ, in leptonic, hadronic, and mixed channels with the result $m_t = 174.30 \pm 0.35_{\rm\,stat.} \pm 0.54_{\rm\,syst.}$ GeV [44]. Likewise, ATLAS (including some $t\bar{t}$ cross section information) and CMS (including results based on alternative techniques) at the LHC obtained $m_t = 172.51 \pm 0.27_{\rm\,stat.} \pm 0.42_{\rm\,syst.}$ GeV [45] and $m_t = 172.43 \pm 0.13_{\rm\,stat.} \pm 0.46_{\rm\,syst.}$ GeV [46], respectively. In addition, CMS obtained a first result with $\sqrt{s} = 13$ TeV data (Run 2) in the lepton + jets channel, $m_t = 172.25 \pm 0.08_{\rm\,mostly\,stat.} \pm 0.62_{\rm\,syst.}$ GeV [47]. Assuming a systematic error component of 0.21 GeV (the QCD, PDF and Monte Carlo type errors at ALTAS) is common to all four determinations, we arrive at the average

$$m_t = 172.74 \pm 0.33_{\rm\,exp.} \pm 0.32_{\rm\,theory}\ \ {\rm GeV}, \tag{10.9}$$

where the last error (taken as the uncertainty [48] in the relation [49] between the $\overline{\rm MS}$ and pole top mass definitions) is meant to account for theoretical uncertainties associated with the precise top mass definition applied in Monte Carlo generators on the one hand, and electroweak radiative correction libraries on the other. It is conceivable that more dedicated treatments [50] of the top mass definition in the future could result in somewhat larger shifts but smaller errors in m_t. The average in Eq. (10.9) differs slightly from the value, $m_t = 173.0 \pm 0.4$ GeV, which appears in the top quark Listings in this *Review* and which is based exclusively on published results. While there seems to be generally good agreement between all these measurements, we observe a 2.8 σ discrepancy (or more in case of correlated systematics) between the two most precise determinations, 174.98 ± 0.76 GeV [51] (by the DØ Collaboration) and 172.25 ± 0.63 GeV [47] (by the CMS Collaboration), both from the lepton + jets channels. For more details, see the Section on "The Top Quark" and the Quarks Listings in this *Review*.

The observables $\sin^2\theta_W$ and M_W can be calculated from M_Z, $\widehat{\alpha}(M_Z)$, and G_F, when values for m_t and M_H are given, or conversely, M_H can be constrained by $\sin^2\theta_W$ and

M_W. The value of $\sin^2\theta_W$ is extracted from neutral-current processes (see Sec. 10.3) and Z pole observables (see Sec. 10.4) and depends on the renormalization prescription. There are a number of popular schemes [52–57] leading to values which differ by small factors depending on m_t and M_H. The notation for these schemes is shown in Table 10.2.

Table 10.2: Notations used to indicate the various schemes discussed in the text. Each definition of $\sin^2\theta_W$ leads to values that differ by small factors depending on m_t and M_H. Numerical values and the uncertainties induced by the imperfectly known SM parameters are also given for illustration.

Scheme	Notation	Value	Parametric uncertainty
On-shell	s^2_W	0.22343	± 0.00007
$\overline{\rm MS}$	$\widehat{s}^2_Z$	0.23122	± 0.00003
$\overline{\rm MS}$ ND	$\widehat{s}^2_{\rm ND}$	0.23142	± 0.00003
$\overline{\rm MS}$	$\widehat{s}^2_0$	0.23857	± 0.00005
Effective angle	$\overline{s}^2_\ell$	0.23154	± 0.00003

(*i*) The on-shell scheme [52] promotes the tree-level formula $\sin^2\theta_W = 1 - M^2_W/M^2_Z$ to a definition of the renormalized $\sin^2\theta_W$ to all orders in perturbation theory, *i.e.*, $\sin^2\theta_W \to s^2_W \equiv 1 - M^2_W/M^2_Z$:

$$M_W = \frac{A_0}{s_W(1-\Delta r)^{1/2}}\ , \qquad M_Z = \frac{M_W}{c_W}\ , \tag{10.10}$$

where $c_W \equiv \cos\theta_W$, $A_0 = (\pi\alpha/\sqrt{2}G_F)^{1/2} = 37.28039(1)$ GeV, and Δr includes the radiative corrections relating α, $\alpha(M_Z)$, G_F, M_W, and M_Z. One finds $\Delta r \sim \Delta r_0 - \rho_t/\tan^2\theta_W$, where $\Delta r_0 = 1 - \alpha/\widehat{\alpha}(M_Z) = 0.06627(8)$ is due to the running of α, and $\rho_t = 3G_F m^2_t/8\sqrt{2}\pi^2 = 0.00935\,(m_t/172.74\ {\rm GeV})^2$ represents the dominant (quadratic) m_t dependence. There are additional contributions to Δr from bosonic loops, including those which depend logarithmically on M_H and higher-order corrections[\$\$]. One has $\Delta r = 0.03672 \mp 0.00017 \pm 0.00008$, where the first uncertainty is from m_t and the second is from $\alpha(M_Z)$. Thus the value of s^2_W extracted from M_Z includes an uncertainty (∓ 0.00005) from the currently allowed range of m_t. This scheme is simple conceptually. However, the relatively large ($\sim 3\%$) correction from ρ_t causes large spurious contributions in higher orders.

s^2_W depends not only on the gauge couplings but also on the spontaneous-symmetry breaking, and it is awkward in the presence of any extension of the SM which perturbs

[\$\$] All explicit numbers quoted here and below include the two- and three-loop corrections described near the end of Sec. 10.2.

the value of M_Z (or M_W). Other definitions are motivated by the tree-level coupling constant definition $\theta_W = \tan^{-1}(g'/g)$:

(*ii*) In particular, the modified minimal subtraction ($\overline{\rm MS}$) scheme introduces the quantity $\sin^2\widehat{\theta}_W(\mu) \equiv \widehat{g}'^2(\mu)/\left[\widehat{g}^{\,2}(\mu) + \widehat{g}'^2(\mu)\right]$, where the couplings $\widehat{g}$ and $\widehat{g}'$ are defined by modified minimal subtraction and the scale μ is conveniently chosen to be M_Z for many EW processes. The value of $\widehat{s}^{\,2}_Z = \sin^2\widehat{\theta}_W(M_Z)$ extracted from M_Z is less sensitive than s^2_W to m_t (by a factor of $\tan^2\theta_W$), and is less sensitive to most types of new physics. It is also very useful for comparing with the predictions of grand unification. There are actually several variant definitions of $\sin^2\widehat{\theta}_W(M_Z)$, differing according to whether or how finite $\alpha\ln(m_t/M_Z)$ terms are decoupled (subtracted from the couplings). One cannot entirely decouple the $\alpha\ln(m_t/M_Z)$ terms from all EW quantities because $m_t \gg m_b$ breaks SU(2) symmetry. The scheme that will be adopted here decouples the $\alpha\ln(m_t/M_Z)$ terms from the γ–Z mixing [18,53], essentially eliminating any $\ln(m_t/M_Z)$ dependence in the formulae for asymmetries at the Z pole when written in terms of $\widehat{s}^{\,2}_Z$. (A similar definition is used for $\widehat{\alpha}$.) The on-shell and $\overline{\rm MS}$ definitions are related by

$$\widehat{s}^{\,2}_Z = c\,(m_t, M_H) s^2_W = (1.0348 \pm 0.0002) s^2_W \ . \tag{10.11}$$

The quadratic m_t dependence is given by $c \sim 1 + \rho_t/\tan^2\theta_W$. The expressions for M_W and M_Z in the $\overline{\rm MS}$ scheme are

$$M_W = \frac{A_0}{\widehat{s}_Z(1-\Delta\widehat{r}_W)^{1/2}} \ , \qquad\qquad M_Z = \frac{M_W}{\widehat{\rho}^{\,1/2}\,\widehat{c}_Z} \ , \tag{10.12}$$

and one predicts $\Delta\widehat{r}_W = 0.06916 \pm 0.00008$. $\Delta\widehat{r}_W$ has no quadratic m_t dependence, because shifts in M_W are absorbed into the observed G_F, so that the error in $\Delta\widehat{r}_W$ is almost entirely due to $\Delta r_0 = 1 - \alpha/\widehat{\alpha}(M_Z)$. The quadratic m_t dependence has been shifted into $\widehat{\rho} \sim 1 + \rho_t$, where including bosonic loops, $\widehat{\rho} = 1.01013 \pm 0.00005$.

(*iii*) A variant $\overline{\rm MS}$ quantity $\widehat{s}^{\,2}_{\rm ND}$ (used in the 1992 edition of this *Review*) does not decouple the $\alpha\ln(m_t/M_Z)$ terms [54]. It is related to $\widehat{s}^{\,2}_Z$ by

$$\widehat{s}^{\,2}_Z = \widehat{s}^{\,2}_{\rm ND}/\left(1 + \frac{\widehat{\alpha}}{\pi}d\right), \tag{10.13a}$$

$$d = \frac{1}{3}\left(\frac{1}{\widehat{s}^{\,2}} - \frac{8}{3}\right)\left[(1 + \frac{\alpha_s}{\pi})\,\ln\frac{m_t}{M_Z} - \frac{15\alpha_s}{8\pi}\right], \tag{10.13b}$$

Thus, $\widehat{s}^{\,2}_Z - \widehat{s}^{\,2}_{\rm ND} = -0.0002$.

(*iv*) Some of the low-energy experiments discussed in the next section are sensitive to the weak mixing angle at almost vanishing momentum transfer (for a review, see Ref. 55). Thus, Table 10.2 also includes $\widehat{s}^{\,2}_0 \equiv \sin^2\widehat{\theta}_W(0)$.

(*v*) Yet another definition, the effective angle [56,57] $\overline{s}^{\,2}_f = \sin\theta^f_{\rm eff}$ for the Z vector coupling to fermion f, is based on Z pole observables and described in Sec. 10.4.

Experiments are at such level of precision that complete one-loop, dominant two-loop, and partial three and four-loop radiative corrections must be applied. For neutral-current and Z pole processes, these corrections are conveniently divided into two classes:

1. QED diagrams involving the emission of real photons or the exchange of virtual photons in loops, but not including vacuum polarization diagrams. These graphs often yield finite and gauge-invariant contributions to observable processes. However, they are dependent on energies, experimental cuts, *etc.*, and must be calculated individually for each experiment.
2. EW corrections, including $\gamma\gamma$, γZ, ZZ, and WW vacuum polarization diagrams, as well as vertex corrections, box graphs, *etc.*, involving virtual W and Z bosons. The one-loop corrections are included for all processes, and many two-loop corrections are also important. In particular, two-loop corrections involving the top quark modify ρ_t in $\widehat{\rho}$, Δr, and elsewhere by

$$\rho_t \to \rho_t[1 + R(M_H, m_t)\rho_t/3]. \tag{10.14}$$

   $R(M_H, m_t)$ can be described as an expansion in M_Z^2/m_t^2, for which the leading m_t^4/M_Z^4 [58] and next-to-leading m_t^2/M_Z^2 [59] terms are known. The complete two-loop calculation of Δr (without further approximation) has been performed in Refs. 60 and 61 for fermionic and purely bosonic diagrams, respectively. Similarly, the EW two-loop calculation for the relation between $\overline{s}_\ell^2$ and s_W^2 is complete [62,63]. More recently, Ref. 64 obtained the $\overline{\rm MS}$ quantities $\Delta\widehat{r}_W$ and $\widehat{\rho}$ to two-loop accuracy, confirming the prediction of M_W in the on-shell scheme from Refs. 61 and 65 within about 4 MeV.

   Mixed QCD-EW contributions to gauge boson self-energies of order $\alpha\alpha_s m_t^2$ [66], $\alpha\alpha_s^2 m_t^2$ [67], and $\alpha\alpha_s^3 m_t^2$ [68] increase the predicted value of m_t by 6%. This is, however, almost entirely an artifact of using the pole mass definition for m_t. The equivalent corrections when using the $\overline{\rm MS}$ definition $\widehat{m}_t(\widehat{m}_t)$ increase m_t by less than 0.5%. The subleading $\alpha\alpha_s$ corrections [69] are also included. Further three-loop corrections of order $\alpha\alpha_s^2$ [70,71], $\alpha^3 m_t^6$, and $\alpha^2\alpha_s m_t^4$ [72], are rather small. The same is true for $\alpha^3 M_H^4$ [73] corrections unless M_H approaches 1 TeV.

   The theoretical uncertainty from unknown higher-order corrections is estimated to amount to 4 MeV for the prediction of M_W [65] and 4.5×10^{-5} for $\overline{s}_\ell^2$ [74].

Throughout this *Review* we utilize EW radiative corrections from the program GAPP [22], which works entirely in the $\overline{\rm MS}$ scheme, and which is independent of the package ZFITTER [57].

10.3. Low energy electroweak observables

In the following we discuss EW precision observables obtained at low momentum transfers [6], *i.e.* $Q^2 \ll M_Z^2$. It is convenient to write the four-fermion interactions relevant to ν-hadron, ν-e, as well as parity violating e-hadron and e-e neutral-current processes in a form that is valid in an arbitrary gauge theory (assuming massless left-handed neutrinos). One has★

$$-\mathscr{L}^{\nu e} = \frac{G_F}{\sqrt{2}}\,\overline{\nu}\gamma_\mu(1-\gamma^5)\nu\;\overline{e}\,\gamma^\mu(g_{LV}^{\nu e} - g_{LA}^{\nu e}\,\gamma^5)e, \tag{10.15}$$

★ We use here slightly different definitions (and to avoid confusion also a different nota-

$$-\mathscr{L}^{\nu h} = \frac{G_F}{\sqrt{2}}\,\overline{\nu}\,\gamma_\mu(1-\gamma^5)\nu\sum_q[g_{LL}^{\nu q}\,\overline{q}\,\gamma^\mu(1-\gamma^5)q + g_{LR}^{\nu q}\,\overline{q}\,\gamma^\mu(1+\gamma^5)q], \tag{10.16}$$

$$-\mathscr{L}^{ee} = -\frac{G_F}{\sqrt{2}}\,g_{AV}^{ee}\,\overline{e}\,\gamma_\mu\gamma^5 e\,\overline{e}\,\gamma^\mu e, \tag{10.17}$$

$$-\mathscr{L}^{eh} = -\frac{G_F}{\sqrt{2}}\sum_q\left[g_{AV}^{eq}\,\overline{e}\,\gamma_\mu\gamma^5 e\,\overline{q}\,\gamma^\mu q + g_{VA}^{eq}\,\overline{e}\,\gamma_\mu e\,\overline{q}\;\gamma^\mu\gamma^5 q\right], \tag{10.18}$$

where one must include the charged-current contribution for ν_e-e and $\overline{\nu}_e$-e and the parity-conserving QED contribution for electron scattering.

The SM tree level expressions for the four-Fermi couplings are given in Table 10.3. Note that they differ from the respective products of the gauge couplings in Eq. (10.5) in the radiative corrections and in the presence of possible physics beyond the SM.

10.3.1. ***Neutrino scattering*** : For a general review on ν-scattering we refer to Ref. 76 (nonstandard neutrino scattering interactions are surveyed in Ref. 77).

The cross-section in the laboratory system for $\nu_\mu e \to \nu_\mu e$ or $\overline{\nu}_\mu e \to \overline{\nu}_\mu e$ elastic scattering [78] is (in this subsection we drop the redundant index L in the effective neutrino couplings)

$$\frac{d\sigma_{\nu,\bar{\nu}}}{dy} = \frac{G_F^2 m_e E_\nu}{2\pi}\left[(g_V^{\nu e} \pm g_A^{\nu e})^2 + (g_V^{\nu e} \mp g_A^{\nu e})^2(1-y)^2 - (g_V^{\nu e 2} - g_A^{\nu e 2})\frac{y\,m_e}{E_\nu}\right], \tag{10.19}$$

where the upper (lower) sign refers to $\nu_\mu(\overline{\nu}_\mu)$, and $y \equiv T_e/E_\nu$ (which runs from 0 to $(1+m_e/2E_\nu)^{-1}$) is the ratio of the kinetic energy of the recoil electron to the incident ν or $\overline{\nu}$ energy. For $E_\nu \gg m_e$ this yields a total cross-section

$$\sigma = \frac{G_F^2 m_e E_\nu}{2\pi}\left[(g_V^{\nu e} \pm g_A^{\nu e})^2 + \frac{1}{3}(g_V^{\nu e} \mp g_A^{\nu e})^2\right]. \tag{10.20}$$

The most accurate measurements [78–81] of $\sin^2\theta_W$ from ν-lepton scattering (see Sec. 10.6) are from the ratio $R \equiv \sigma_{\nu_\mu e}/\sigma_{\overline{\nu}_\mu e}$, in which many of the systematic uncertainties cancel. Radiative corrections (other than m_t effects) are small compared to the precision of present experiments and have negligible effect on the extracted $\sin^2\theta_W$. The most precise experiment (CHARM II) [79] determined not only $\sin^2\theta_W$ but $g_{V,A}^{\nu e}$ as well, which are shown in Fig. 10.1. The cross-sections for ν_e-e and $\overline{\nu}_e$-e may be obtained from Eq. (10.19) by replacing $g_{V,A}^{\nu e}$ by $g_{V,A}^{\nu e} + 1$, where the 1 is due to the charged-current contribution.

---

tion) for the coefficients of these four-Fermi operators than we did in previous editions of this *Review*. The new couplings [75] are defined in the static limit, $Q^2 \to 0$, with specific radiative corrections included, while others (more experiment specific ones) are assumed to be removed by the experimentalist. They are convenient in that their determinations from very different types of processes can be straightforwardly combined.

Table 10.3: SM tree level expressions for the neutral-current parameters for ν-hadron, ν-e, and e^--scattering processes. To obtain the SM values in the last column, the tree level expressions have to be multiplied by the low-energy neutral-current ρ parameter, $\rho_{\rm NC} = 1.00058$, and further vertex and box corrections need to be added as detailed in Ref. 75. The dominant m_t dependence is again given by $\rho_{\rm NC} \sim 1 + \rho_t$.

Quantity	SM tree level	SM value
$g_{LV}^{\nu_\mu e}$	$-\frac{1}{2} + 2\,\widehat{s}_0^2$	-0.0398
$g_{LA}^{\nu_\mu e}$	$-\frac{1}{2}$	-0.5063
$g_{LL}^{\nu_\mu u}$	$\frac{1}{2} - \frac{2}{3}\,\widehat{s}_0^2$	0.3458
$g_{LL}^{\nu_\mu d}$	$-\frac{1}{2} + \frac{1}{3}\,\widehat{s}_0^2$	-0.4288
$g_{LR}^{\nu_\mu u}$	$-\frac{2}{3}\,\widehat{s}_0^2$	-0.1552
$g_{LR}^{\nu_\mu d}$	$\frac{1}{3}\,\widehat{s}_0^2$	0.0777
g_{AV}^{ee}	$\frac{1}{2} - 2\,\widehat{s}_0^2$	0.0226
g_{AV}^{eu}	$-\frac{1}{2} + \frac{4}{3}\,\widehat{s}_0^2$	-0.1888
g_{AV}^{ed}	$\frac{1}{2} - \frac{2}{3}\,\widehat{s}_0^2$	0.3419
g_{VA}^{eu}	$-\frac{1}{2} + 2\,\widehat{s}_0^2$	-0.0352
g_{VA}^{ed}	$\frac{1}{2} - 2\,\widehat{s}_0^2$	0.0249

A precise determination of the on-shell s_W^2, which depends only very weakly on m_t and M_H, is obtained from deep inelastic scattering (DIS) of neutrinos from (approximately) isoscalar targets [82]. The ratio $R_\nu \equiv \sigma_{\nu N}^{NC}/\sigma_{\nu N}^{CC}$ of neutral-to-charged-current cross-sections has been measured to 1% accuracy by CDHS [83] and CHARM [84] at CERN. CCFR [85] at Fermilab has obtained an even more precise result, so it is important to obtain theoretical expressions for R_ν and $R_{\bar\nu} \equiv \sigma_{\bar\nu N}^{NC}/\sigma_{\bar\nu N}^{CC}$ to comparable accuracy. Fortunately, many of the uncertainties from the strong interactions and neutrino spectra cancel in the ratio. A large theoretical uncertainty is associated with the c-threshold, which mainly affects σ^{CC}. Using the slow rescaling prescription [86] the central value of $\sin^2\theta_W$ from CCFR varies as $0.0111(m_c/\text{GeV} - 1.31)$, where m_c is the effective mass which is numerically close to the $\overline{\rm MS}$ mass $\widehat{m}_c(\widehat{m}_c)$, but their exact relation is unknown at higher orders. For $m_c = 1.31 \pm 0.24$ GeV (determined from ν-induced dimuon production [87]) this contributes ± 0.003 to the total uncertainty $\Delta \sin^2\theta_W \sim \pm 0.004$.

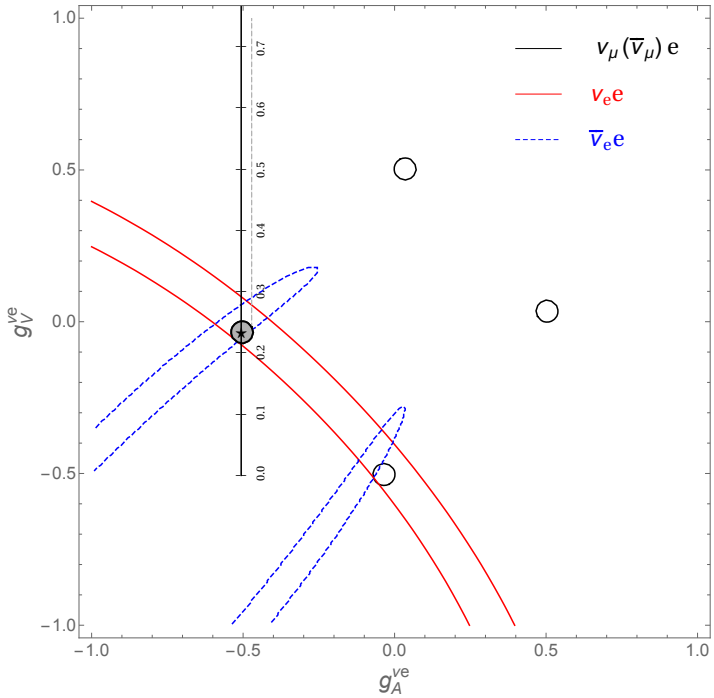

Figure 10.1: Allowed contours in $g_A^{\nu e}$ *vs.* $g_V^{\nu e}$ from neutrino-electron scattering and the SM prediction as a function of $\widehat{s}^2_Z$. (The SM best fit value $\widehat{s}^2_Z = 0.23122$ is also indicated.) The $\nu_e e$ [80] and $\bar{\nu}_e e$ [81] constraints are at 1 σ, while each of the four equivalent $\nu_\mu(\bar{\nu}_\mu)e$ [78–79] solutions ($g_{V,A} \to -g_{V,A}$ and $g_{V,A} \to g_{A,V}$) are at the 90% C.L. The global best fit region (shaded) almost exactly coincides with the corresponding $\nu_\mu(\bar{\nu}_\mu)e$ region. The solution near $g_A = 0, g_V = -0.5$ is eliminated by $e^+e^- \to \ell^+\ell^-$ data under the weak additional assumption that the neutral current is dominated by the exchange of a single Z boson.

(The experimental uncertainty is also ± 0.003.) This uncertainty largely cancels, however, in the Paschos-Wolfenstein ratio [88],

$$R^- = \frac{\sigma^{NC}_{\nu N} - \sigma^{NC}_{\bar{\nu} N}}{\sigma^{CC}_{\nu N} - \sigma^{CC}_{\bar{\nu} N}} \ . \tag{10.21}$$

It was measured by Fermilab's NuTeV collaboration [89] for the first time, and required a high-intensity and high-energy anti-neutrino beam.

A simple zero$^{\text{th}}$-order approximation is

$$R_\nu = g_L^2 + g_R^2 r \ , \qquad R_{\bar{\nu}} = g_L^2 + \frac{g_R^2}{r} \ , \qquad R^- = g_L^2 - g_R^2 \ , \tag{10.22}$$

where

$$g_L^2 \equiv (g_{LL}^{\nu_\mu u})^2 + (g_{LL}^{\nu_\mu d})^2 \approx \frac{1}{2} - \sin^2\theta_W + \frac{5}{9}\sin^4\theta_W, \tag{10.23a}$$

$$g_R^2 \equiv (g_{LR}^{\nu_\mu u})^2 + (g_{LR}^{\nu_\mu d})^2 \approx \frac{5}{9}\sin^4\theta_W, \tag{10.23b}$$

and $r \equiv \sigma^{CC}_{\overline{\nu}N}/\sigma^{CC}_{\nu N}$ is the ratio of $\overline{\nu}$ to ν charged-current cross-sections, which can be measured directly. [In the simple parton model, ignoring hadron energy cuts, $r \approx (\frac{1}{3}+\epsilon)/(1+\frac{1}{3}\epsilon)$, where $\epsilon \sim 0.125$ is the ratio of the fraction of the nucleon's momentum carried by anti-quarks to that carried by quarks.] In practice, Eq. (10.22) must be corrected for quark mixing, quark sea effects, c-quark threshold effects, non-isoscalarity, W–Z propagator differences, the finite muon mass, QED and EW radiative corrections. Details of the neutrino spectra, experimental cuts, x and Q^2 dependence of structure functions, and longitudinal structure functions enter only at the level of these corrections and therefore lead to very small uncertainties. CCFR quotes $s^2_W = 0.2236 \pm 0.0041$ for $(m_t, M_H) = (175, 150)$ GeV with very little sensitivity to (m_t, M_H).

The NuTeV collaboration found $s^2_W = 0.2277 \pm 0.0016$ (for the same reference values), which was 3.0 σ higher than the SM prediction [89]. However, since then several groups have raised concerns about interpretation of the NuTeV result, which could affect the extracted $g^2_{L,R}$ (and thus s^2_W) including their uncertainties and correlation. These include the assumption of symmetric strange and antistrange sea quark distributions, the electron neutrino contamination from K_{e3} decays, isospin symmetry violation in the parton distribution functions and from QED splitting effects, nuclear shadowing effects, and a more complete treatment of EW and QCD radiative corrections. A more detailed discussion and a list of references can be found in the 2016 edition of this *Review*. The precise impact of these effects would need to be evaluated carefully by the collaboration, but in the absence of a such an effort we do not include the νDIS constraints in our default set of fits.

10.3.2. ***Parity violation*** : For a review on weak polarized electron scattering we refer to Ref. 90. The SLAC polarized electron-deuteron DIS (eDIS) experiment [91] measured the right-left asymmetry,

$$A = \frac{\sigma_R - \sigma_L}{\sigma_R + \sigma_L} \ , \tag{10.24}$$

where $\sigma_{R,L}$ is the cross-section for the deep-inelastic scattering of a right- or left-handed electron: $e_{R,L}N \to e\mathrm{X}$. In the quark parton model,

$$\frac{A}{Q^2} = a_1 + a_2 \frac{1-(1-y)^2}{1+(1-y)^2} \ , \tag{10.25}$$

where $Q^2 > 0$ is the momentum transfer and y is the fractional energy transfer from the electron to the hadrons. For the deuteron or other isoscalar targets, one has, neglecting the s-quark and anti-quarks,

$$a_1 = \frac{3G_F}{5\sqrt{2}\pi\alpha}\left(g^{eu}_{AV} - \frac{1}{2}g^{ed}_{AV}\right) \approx \frac{3G_F}{5\sqrt{2}\pi\alpha}\left(-\frac{3}{4} + \frac{5}{3}\widehat{s}^2_0\right), \tag{10.26a}$$

$$a_2 = \frac{3G_F}{5\sqrt{2}\pi\alpha}\left(g^{eu}_{VA} - \frac{1}{2}g^{ed}_{VA}\right) \approx \frac{9G_F}{5\sqrt{2}\pi\alpha}\left(\widehat{s}^2_0 - \frac{1}{4}\right). \tag{10.26b}$$

The Jefferson Lab Hall A Collaboration [92] improved on the SLAC result by determining A at $Q^2 = 1.085$ GeV and 1.901 GeV, and determined the weak mixing angle to 2% precision. In another polarized-electron scattering experiment on deuterons, but in the quasi-elastic kinematic regime, the SAMPLE experiment [93] at MIT-Bates extracted the combination $g_{VA}^{eu} - g_{VA}^{ed}$ at Q^2 values of 0.1 GeV^2 and 0.038 GeV^2. What was actually determined were nucleon form factors from which the quoted results were obtained by the removal of a multi-quark radiative correction [94]. Other linear combinations of the effective couplings have been determined in polarized-lepton scattering at CERN in μ-C DIS, at Mainz in e-Be (quasi-elastic), and at Bates in e-C (elastic). See the review articles in Refs. 95 and 96 for more details. Recent polarized electron scattering experiments, *i.e.*, SAMPLE, the PVA4 experiment at Mainz, and the HAPPEX and GØ experiments at Jefferson Lab, have focussed on the strange quark content of the nucleon. These are reviewed in Refs. 97 and 98.

The parity violating asymmetry, A_{PV}, in fixed target polarized Møller scattering, $e^-e^- \to e^-e^-$, is defined as in Eq. (10.24) and reads [99],

$$\frac{A_{PV}}{Q^2} = -2\, g_{AV}^{ee} \frac{G_F}{\sqrt{2}\pi\alpha} \frac{1-y}{1+y^4+(1-y)^4} \ , \tag{10.27}$$

where y is again the energy transfer. It has been measured at low $Q^2 = 0.026$ GeV^2 in the SLAC E158 experiment [100], with the result $A_{PV} = (-1.31 \pm 0.14_{\rm stat.} \pm 0.10_{\rm syst.}) \times 10^{-7}$. Expressed in terms of the weak mixing angle in the $\overline{\rm MS}$ scheme, this yields $\widehat{s}^2(Q^2) = 0.2403 \pm 0.0013$, and established the scale dependence of the weak mixing angle (see $Q_W(e)$ in Fig. 10.2) at the level of 6.4 σ. One can also extract the model-independent effective coupling, $g_{AV}^{ee} = 0.0190 \pm 0.0027$ [75] (the implications are discussed in Ref. 103).

In a similar experiment and at about the same $Q^2 = 0.025$ GeV^2, Qweak at Jefferson Lab [106] measured the weak charge of the proton (which is proportional to $2g_{AV}^{eu} + g_{AV}^{ed}$) and $\sin^2\theta_W$ in polarized ep scattering with relative precisions of 6% and 0.5%, respectively. The preliminary result [107] based on the full data set corresponds to the constraint $2g_{AV}^{eu} + g_{AV}^{ed} = 0.0356 \pm 0.0023$, and to a measurement of the weak mixing angle, $\widehat{s}^2(Q^2) = 0.2382 \pm 0.0011$.

There are precise experiments measuring atomic parity violation (APV) [108,109] in cesium [110,111] (at the 0.4% level [110]), thallium [112], lead [113], and bismuth [114]. The EW physics is contained in the nuclear weak charges $Q_W^{Z,N}$, where Z and N are the numbers of protons and neutrons in the nucleus. In terms of the nucleon vector couplings,

$$g_{AV}^{ep} \equiv 2g_{AV}^{eu} + g_{AV}^{ed} \approx -\frac{1}{2} + 2\widehat{s}_0^2, \tag{10.28}$$

$$g_{AV}^{en} \equiv g_{AV}^{eu} + 2g_{AV}^{ed} \approx \frac{1}{2}, \tag{10.29}$$

one has,

$$Q_W^{Z,N} \equiv -2\left[Z(g_{AV}^{ep} + 0.00005) + N(g_{AV}^{en} + 0.00006)\right]\left(1 - \frac{\alpha}{2\pi}\right), \tag{10.30}$$

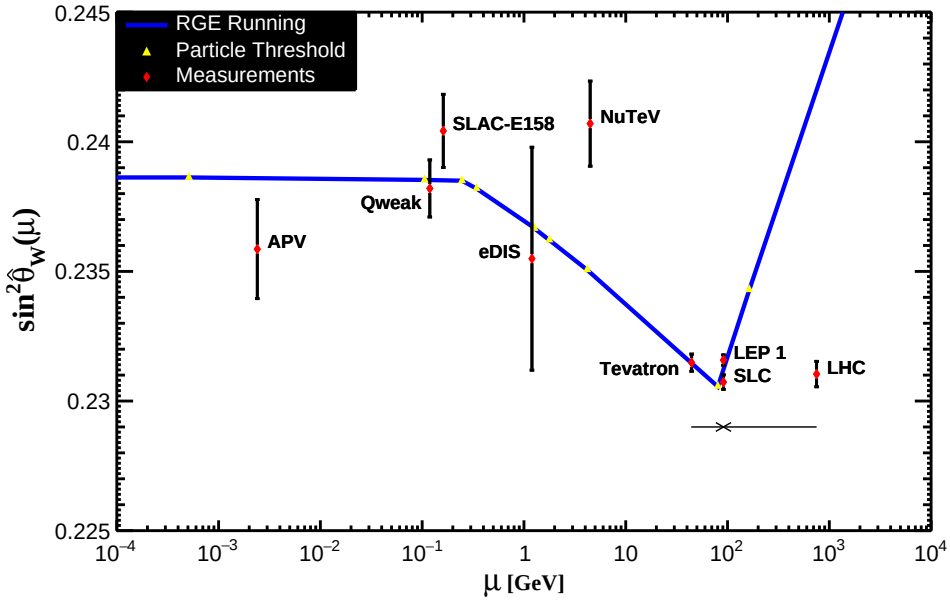

Figure 10.2: Scale dependence of the weak mixing angle defined in the $\overline{\rm MS}$ scheme [101,102] (for the scale dependence of the weak mixing angle defined in a mass-dependent renormalization scheme, see Ref. 103). The minimum of the curve corresponds to $\mu = M_W$, below which we switch to an effective theory with the $W^\pm$ bosons integrated out, and where the β-function for the weak mixing angle changes sign. At the location of the W boson mass and each fermion mass there are also discontinuities arising from scheme dependent matching terms which are necessary to ensure that the various effective field theories within a given loop order describe the same physics. However, in the $\overline{\rm MS}$ scheme these are very small numerically and barely visible in the figure provided one decouples quarks at $\mu = \widehat{m}_q(\widehat{m}_q)$. The width of the curve exceeds the theory uncertainty from strong interaction effects which at low energies is at the level of $\pm 2 \times 10^{-5}$ [102]. Following the estimate [104] of the typical momentum transfer for parity violation experiments in Cs, the location of the APV data point is given by $\mu = 2.4$ MeV. For NuTeV we display the updated value from Ref. 105 and chose $\mu = \sqrt{20}$ GeV which is about half-way between the averages of $\sqrt{Q^2}$ for ν and $\overline{\nu}$ interactions at NuTeV. The Tevatron and LHC measurements are strongly dominated by invariant masses of the final state dilepton pair of $\mathcal{O}(M_Z)$ and can thus be considered as additional Z pole data points. For clarity we displayed the Tevatron and LHC points horizontally to the left and to the right, respectively.

where the numerically small adjustments are discussed in Ref. 75 and include the result of the γZ-box correction from Ref. 115. *E.g.*, $Q_W(^{133}\mathrm{Cs})$ is extracted by measuring experimentally the ratio of the parity violating amplitude, $E_{\rm PNC}$, to the Stark vector transition polarizability, β, and by calculating theoretically $E_{\rm PNC}$ in terms of Q_W. One

can then write,

$$Q_W = N \left(\frac{\mathrm{Im}\, E_{\mathrm{PNC}}}{\beta}\right)_{\mathrm{exp.}} \left(\frac{|e|\, a_B}{\mathrm{Im}\, E_{\mathrm{PNC}}} \frac{Q_W}{N}\right)_{\mathrm{th.}} \left(\frac{\beta}{a_B^3}\right)_{\mathrm{exp.+th.}} \left(\frac{a_B^2}{|e|}\right),$$

where a_B is the Bohr radius. The uncertainties associated with atomic wave functions are quite small for cesium [116]. The semi-empirical value of β used in early analyses added another source of theoretical uncertainty [117]. However, the ratio of the off-diagonal hyperfine amplitude to the polarizability was subsequently measured directly by the Boulder group [118]. Combined with the precisely known hyperfine amplitude [119] one finds $\beta = (26.991 \pm 0.046)\, a_B^3$, in excellent agreement with the earlier results, reducing the overall theory uncertainty (while slightly increasing the experimental error). Utilizing the state-of-the-art many-body calculation in Ref. 120 yields $\mathrm{Im}\, E_{\mathrm{PNC}} = (0.8906 \pm 0.0026) \times 10^{-11} |e|\, a_B\, Q_W/N$, while the two measurements [110,111] combine to give $\mathrm{Im}\, E_{\mathrm{PNC}}/\beta = -1.5924 \pm 0.0055$ mV/cm, and we would obtain $Q_W(^{133}_{78}\mathrm{Cs}) = -73.20 \pm 0.35$, or equivalently $55 g_{AV}^{ep} + 78 g_{AV}^{en} = 36.64 \pm 0.18$ which is in excellent agreement with the SM prediction of 36.65. However, a very recent atomic structure calculation [121] found significant corrections to two non-dominating terms, changing the result to $\mathrm{Im}\, E_{\mathrm{PNC}} = (0.8977 \pm 0.0040) \times 10^{-11} |e|\, a_B\, Q_W/N$, and yielding the constraint, $55 g_{AV}^{ep} + 78 g_{AV}^{en} = 36.35 \pm 0.21$ [$Q_W(^{133}_{78}\mathrm{Cs}) = -72.62 \pm 0.43$], *i.e.* a 1.5 σ SM deviation. Thus, the various theoretical efforts in [120–122] together with an update of the SM calculation [123] reduced an earlier 2.3 σ discrepancy from the SM (see the year 2000 edition of this *Review*), but there still appears to remain a small deviation. The theoretical uncertainties are 3% for thallium [124] but larger for the other atoms. The Boulder experiment in cesium also observed the parity-violating weak corrections to the nuclear electromagnetic vertex (the anapole moment [125]) .

In the future it could be possible to further reduce the theoretical wave function uncertainties by taking the ratios of parity violation in different isotopes [108,126]. There would still be some residual uncertainties from differences in the neutron charge radii, however [127]. Experiments in hydrogen and deuterium are another possibility for reducing the atomic theory uncertainties [128], while measurements of single trapped radium ions are promising [129] because of the much larger parity violating effect.

10.4. Physics of the massive electroweak bosons

If the CM energy $\sqrt{s}$ is large compared to the fermion mass m_f, the unpolarized Born cross-section for $e^+e^- \to f\bar{f}$ can be written as

$$\frac{d\sigma}{d\cos\theta} = \frac{\pi\alpha^2(s)}{2s}\left[F_1(1+\cos^2\theta) + 2F_2\cos\theta\right] + B, \qquad (10.31a)$$

where

$$F_1 = Q_e^2 Q_f^2 - 2\chi Q_e Q_f \overline{g}_V^e \overline{g}_V^f \cos\delta_R + \chi^2 (\overline{g}_V^{e2} + \overline{g}_A^{e2})(\overline{g}_V^{f2} + \overline{g}_A^{f2}) \qquad (10.31b)$$

$$F_2 = -2\chi\, Q_e Q_f \overline{g}_A^e \overline{g}_A^f \cos\delta_R + 4\chi^2 \overline{g}_V^e \overline{g}_A^e \overline{g}_V^f \overline{g}_A^f \tag{10.31c}$$

$$\tan\delta_R = \frac{\overline{M}_Z \overline{\Gamma}_Z}{\overline{M}_Z^2 - s}\ , \qquad \chi = \frac{G_F}{2\sqrt{2}\pi\alpha(s)} \frac{s\overline{M}_Z^2}{\left[(\overline{M}_Z^2 - s)^2 + \overline{M}_Z^2 \overline{\Gamma}_Z^2\right]^{1/2}}\ , \tag{10.32}$$

B accounts for box graphs involving virtual Z and W bosons, and the $\overline{g}_{V,A}^f$ are defined in Eq. (10.33) below. $\overline{M}_Z$ and $\overline{\Gamma}_Z$ correspond to mass and width definitions based on a Breit-Wigner shape with an energy-independent width (see the Section on "The Z Boson" in the Gauge and Higgs Boson Particle Listings of this *Review*). The differential cross-section receives important corrections from QED effects in the initial and final state, and interference between the two (see *e.g.* Ref. 130). For $q\bar{q}$ production, there are additional final-state QCD corrections, which are relatively large. Note also that the equations above are written in the CM frame of the incident e^+e^- system, which may be boosted due to the initial-state QED radiation.

Some of the leading virtual EW corrections are captured by the running QED coupling $\alpha(s)$ and the Fermi constant G_F. The remaining corrections to the $Zf\bar{f}$ interaction are absorbed by replacing the tree-level couplings in Eq. (10.5) with the s-dependent *effective couplings* [131],

$$\overline{g}_V^f = \sqrt{\rho_f}\,(t_{3L}^{(f)} - 2Q_f \kappa_f \sin^2\theta_W), \qquad \overline{g}_A^f = \sqrt{\rho_f}\, t_{3L}^{(f)}. \tag{10.33}$$

In these equations, the effective couplings are to be taken at the scale $\sqrt{s}$, but for notational simplicity we do not show this explicitly. At tree-level $\rho_f = \kappa_f = 1$, but inclusion of EW radiative corrections leads to non-zero $\rho_f - 1$ and $\kappa_f - 1$, which depend on the fermion f and on the renormalization scheme. In the on-shell scheme, the quadratic m_t dependence is given by $\rho_f \sim 1 + \rho_t$, $\kappa_f \sim 1 + \rho_t/\tan^2\theta_W$, while in $\overline{\rm MS}$, $\widehat{\rho}_f \sim \widehat{\kappa}_f \sim 1$, for $f \neq b$ ($\widehat{\rho}_b \sim 1 - \frac{4}{3}\rho_t$, $\widehat{\kappa}_b \sim 1 + \frac{2}{3}\rho_t$). In the $\overline{\rm MS}$ scheme the normalization is changed according to $G_F M_Z^2/2\sqrt{2}\pi \to \widehat{\alpha}/4\widehat{s}_Z^2\widehat{c}_Z^2$ in Eq. (10.32).

For the high-precision Z-pole observables discussed below, additional bosonic and fermionic loops, vertex corrections, and higher order contributions, *etc.*, must be included [62,63,132–134]. For example, in the $\overline{\rm MS}$ scheme one has $\widehat{\rho}_\ell = 0.9977$, $\widehat{\kappa}_\ell = 1.0014$, $\widehat{\rho}_b = 0.9868$, and $\widehat{\kappa}_b = 1.0068$.

To connect to measured quantities, it is convenient to define an effective angle $\overline{s}_f^2 \equiv \sin^2\overline{\theta}_{Wf} \equiv \widehat{\kappa}_f \widehat{s}_Z^2 = \kappa_f s_W^2$, in terms of which $\overline{g}_V^f$ and $\overline{g}_A^f$ are given by $\sqrt{\rho_f}$ times their tree-level formulae. One finds that the $\widehat{\kappa}_f$ ($f \neq b$) are almost independent of (m_t, M_H), and thus one can write

$$\overline{s}_\ell^2 = \widehat{s}_Z^2 + 0.00032, \tag{10.34}$$

while the κ's for the other schemes are m_t dependent.

10.4.1. e^+e^- *scattering below the Z pole* :

Experiments at PEP, PETRA and TRISTAN have measured the unpolarized forward-backward asymmetry, A_{FB}, and the total cross-section relative to pure QED, R, for $e^+e^- \to \ell^+\ell^-$, $\ell = \mu$ or τ at CM energies $\sqrt{s} < M_Z$. They are defined as

$$A_{FB} \equiv \frac{\sigma_F - \sigma_B}{\sigma_F + \sigma_B} \ , \qquad R = \frac{\sigma}{\mathcal{R}_{\rm ini} 4\pi\alpha^2/3s} \ , \tag{10.35}$$

where $\sigma_F\,(\sigma_B)$ is the cross-section for ℓ^- to travel forward (backward) with respect to the e^- direction. Neglecting box graph contribution, they are given by

$$A_{FB} = \frac{3}{4}\frac{F_2}{F_1} \ , \qquad R = F_1 \ . \tag{10.36}$$

For the available data, it is sufficient to approximate the EW corrections through the leading running $\alpha(s)$ and quadratic m_t contributions [135,136] as described above. Reviews and formulae for $e^+e^- \to$ hadrons may be found in Ref. 137.

10.4.2. *Z pole physics* :

High-precision measurements of various Z pole ($\sqrt{s} \approx M_Z$) observables have been performed at LEP 1 and SLC [10,138–143], as summarized in Table 10.5. These include the Z mass and total width, Γ_Z, and partial widths $\Gamma(f\overline{f})$ for $Z \to f\overline{f}$, where $f = e,\ \mu,\ \tau$, light hadrons, b, or c. It is convenient to use the variables $M_Z,\ \Gamma_Z,\ R_\ell \equiv \Gamma({\rm had})/\Gamma(\ell^+\ell^-)$ $(\ell = e, \mu, \tau)$, $\sigma_{\rm had} \equiv 12\pi\,\Gamma(e^+e^-)\,\Gamma({\rm had})/M_Z^2\,\Gamma_Z^{2\,\dagger\dagger}$, $R_b \equiv \Gamma(b\overline{b})/\Gamma({\rm had})$, and $R_c \equiv \Gamma(c\overline{c})/\Gamma({\rm had})$, most of which are weakly correlated experimentally. ($\Gamma({\rm had})$ is the partial width into hadrons.) The three values for R_ℓ are consistent with lepton universality (although R_τ is somewhat low compared to R_e and R_μ), but we use the general analysis in which the three observables are treated as independent. Similar remarks apply to $A_{FB}^{0,\ell}$ defined through Eq. (10.39) with $P_e = 0$ ($A_{FB}^{0,\tau}$ is somewhat high). $\mathcal{O}(\alpha^3)$ QED corrections introduce a large anti-correlation (-30%) between Γ_Z and $\sigma_{\rm had}$. The anti-correlation between R_b and R_c is -18% [10]. The R_ℓ are insensitive to m_t except for the $Z \to b\overline{b}$ vertex and final state corrections and the implicit dependence through $\sin^2\theta_W$. Thus, they are especially useful for constraining α_s. The invisible decay width [10], $\Gamma({\rm inv}) = \Gamma_Z - 3\,\Gamma(\ell^+\ell^-) - \Gamma({\rm had}) = 499.0 \pm 1.5$ MeV, can be used to determine the number of neutrino flavors, $N_\nu = \Gamma({\rm inv})/\Gamma^{\rm theory}(\nu\overline{\nu})$, much lighter than $M_Z/2$. In practice, we determine N_ν by allowing it as an additional fit parameter and obtain,

$$N_\nu = 2.991 \pm 0.007 \ . \tag{10.37}$$

Additional constraints follow from measurements of various Z-pole asymmetries. These include the forward-backward asymmetry A_{FB} and the polarization or left-right asymmetry,

$$A_{LR} \equiv \frac{\sigma_L - \sigma_R}{\sigma_L + \sigma_R} \ , \tag{10.38}$$

†† Note that $\sigma_{\rm had}$ receives additional EW corrections that are not captured in the partial widths [134,144], but they only enter at two-loop order.

where $\sigma_L(\sigma_R)$ is the cross-section for a left-(right-)handed incident electron. A_{LR} was measured precisely by the SLD collaboration at the SLC [140], and has the advantages of being very sensitive to $\sin^2\theta_W$ and that systematic uncertainties largely cancel. After removing initial state QED corrections and contributions from photon exchange, γ–Z interference and EW boxes, see Eq. (10.31), one can use the effective tree-level expressions

$$A_{LR} = A_e P_e \ , \qquad A_{FB} = \frac{3}{4} A_f \, \frac{A_e + P_e}{1 + P_e A_e} \ , \tag{10.39}$$

where

$$A_f \equiv \frac{2\overline{g}_V^f \, \overline{g}_A^f}{\overline{g}_V^{f2} + \overline{g}_A^{f2}} = \frac{1 - 4|Q_f|\bar{s}_f^2}{1 - 4|Q_f|\bar{s}_f^2 + 8(|Q_f|\bar{s}_f^2)^2} \ . \tag{10.40}$$

P_e is the initial e^- polarization, so that the second equality in Eq. (10.41) is reproduced for $P_e = 1$, and the Z pole forward-backward asymmetries at LEP 1 ($P_e = 0$) are given by $A_{FB}^{(0,f)} = \frac{3}{4} A_e A_f$ where $f = e,\ \mu,\ \tau,\ b,\ c,\ s$ [10], and q, and where $A_{FB}^{(0,q)}$ refers to the hadronic charge asymmetry. Corrections for t-channel exchange and s/t-channel interference cause $A_{FB}^{(0,e)}$ to be strongly anti-correlated with R_e (-37%). The correlation between $A_{FB}^{(0,b)}$ and $A_{FB}^{(0,c)}$ amounts to 15%.

In addition, SLD extracted the final-state couplings A_b, A_c [10], A_s [141], A_τ, and A_μ [142], from left-right forward-backward asymmetries, using

$$A_{LR}^{FB}(f) = \frac{\sigma_{LF}^f - \sigma_{LB}^f - \sigma_{RF}^f + \sigma_{RB}^f}{\sigma_{LF}^f + \sigma_{LB}^f + \sigma_{RF}^f + \sigma_{RB}^f} = \frac{3}{4} A_f \ , \tag{10.41}$$

where, for example, σ_{LF}^f is the cross-section for a left-handed incident electron to produce a fermion f traveling in the forward hemisphere. Similarly, A_τ and A_e were measured at LEP 1 [10] through the τ polarization, $\mathcal{P}_\tau$, as a function of the scattering angle θ, which can be written as

$$\mathcal{P}_\tau = -\frac{A_\tau(1 + \cos^2\theta) + 2A_e \cos\theta}{(1 + \cos^2\theta) + 2A_\tau A_e \cos\theta} \tag{10.42}$$

The average polarization, $\langle \mathcal{P}_\tau \rangle$, obtained by integrating over $\cos\theta$ in the numerator and denominator of Eq. (10.42), yields $\langle \mathcal{P}_\tau \rangle = -A_\tau$, while A_e can be extracted from the angular distribution of $\mathcal{P}_\tau$.

The initial state coupling, A_e, was also determined through the left-right charge asymmetry [143] and in polarized Bhabba scattering [142] at SLC. Because $\overline{g}_V^\ell$ is very small, not only $A_{LR}^0 = A_e$, $A_{FB}^{(0,\ell)}$, and $\mathcal{P}_\tau$, but also $A_{FB}^{(0,b)}$, $A_{FB}^{(0,c)}$, $A_{FB}^{(0,s)}$, and the hadronic asymmetries are mainly sensitive to $\overline{s}_\ell^2$.

As mentioned in Sec. 10.2, radiative corrections to $\bar{s}_\ell^2$ have been computed with full two-loop and partial higher-order corrections. The same level of accuracy is available for $\bar{s}_b^2$ [133], while for $\bar{s}_{s,c}$ [74] the purely bosonic contributions of this order are still missing. Similarly, for the partial widths, $\Gamma(f\overline{f})$, and the hadronic peak cross-section,

$\sigma_{\rm had}$, the fermionic two-loop EW corrections are known [134]. Non-factorizable $\mathcal{O}(\alpha\alpha_s)$ corrections to the $Z \to q\bar{q}$ vertex are also available [132]. They add coherently, resulting in a sizable effect and shift $\alpha_s(M_Z)$ when extracted from Z lineshape observables by $\approx +0.0007$. As an example of the precision of the Z-pole observables, the values of $\bar{g}_A^f$ and $\bar{g}_V^f$, $f = e, \mu, \tau, \ell$, extracted from the LEP and SLC lineshape and asymmetry data, are shown in Fig. 10.3, which should be compared with Fig. 10.1. (The two sets of parameters coincide in the SM at tree-level.)

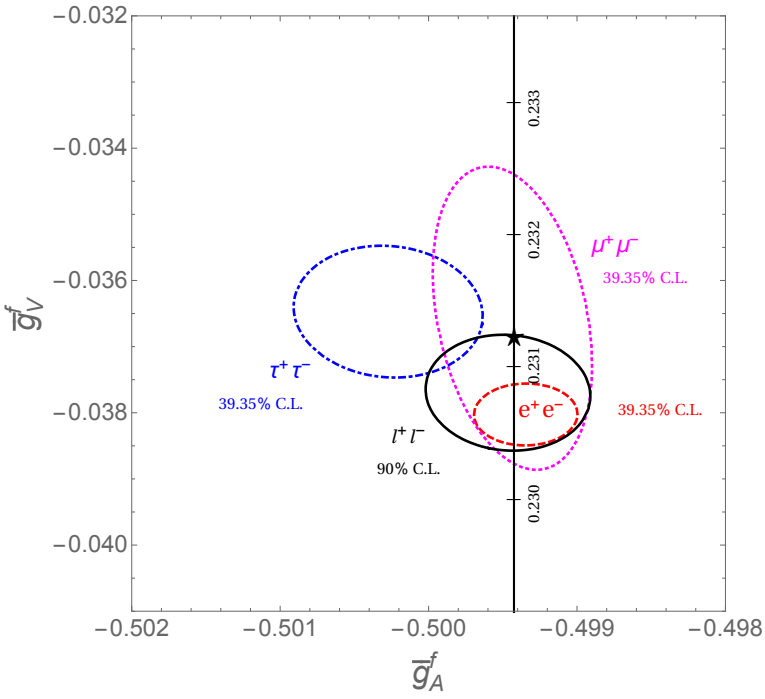

Figure 10.3: 1 σ (39.35% C.L.) contours for the Z-pole observables $\bar{g}_A^f$ and $\bar{g}_V^f$, $f = e, \mu, \tau$ obtained at LEP and SLC [10], compared to the SM expectation as a function of $\widehat{s}^2_Z$. (The SM best fit value $\widehat{s}^2_Z = 0.23122$ is also indicated.) Also shown is the 90% CL allowed region in $\bar{g}^\ell_{A,V}$ obtained assuming lepton universality.

As for hadron colliders, the forward-backward asymmetry, A_{FB}, for e^+e^- and $\mu^+\mu^-$ final states (with invariant masses restricted to or dominated by values around M_Z) in $p\bar{p}$ collisions has been measured by the CDF [145] and DØ [146] collaborations, and the values $\overline{s}^2_\ell = 0.23221 \pm 0.00046$ and $\overline{s}^2_\ell = 0.23095 \pm 0.00040$ were extracted, respectively. The combination of these measurements yields [147]

$$\overline{s}^2_\ell = 0.23148 \pm 0.00033 \text{ (Tevatron)}. \tag{10.43}$$

By varying the invariant mass and the scattering angle (and assuming the electron couplings), information on the effective Z couplings to light quarks, $\overline{g}^{u,d}_{V,A}$, could also be obtained [148,149], but with large uncertainties and mutual correlations and not

independently of $\overline{s}^2_\ell$ above. Similar analyses have also been reported by the H1 [150] and ZEUS [151] collaborations at HERA and by the LEP collaborations [10]. This kind of measurement is harder in the pp environment due to the difficulty to assign the initial quark and antiquark in the underlying Drell-Yan process to the protons. Nevertheless, measurements of A_{FB} have been reported by the ATLAS [152], CMS [153] and LHCb [154] collaborations (the latter only for the $\mu^+\mu^-$ final state), which obtained $\overline{s}^2_\ell = 0.2308 \pm 0.0012$, $\overline{s}^2_\ell = 0.23101 \pm 0.00052$ and $\overline{s}^2_\ell = 0.23142 \pm 0.00106$, respectively. Assuming that the smallest theoretical uncertainty (± 0.00034 from CMS [153]) is fully correlated among all three experiments, these measurements combine to

$$\overline{s}^2_\ell = 0.23104 \pm 0.00049 \text{ (LHC)}, \tag{10.44}$$

in perfect agreement with DØ, but lower than the value found by CDF.

10.4.3. *LEP 2* :

LEP 2 [155,156] ran at several energies above the Z pole up to $\sim$ 209 GeV. Measurements were made of a number of observables, including the cross-sections for $e^+e^- \to f\bar{f}$ for $f = q, \mu, \tau$; the differential cross-sections for $f = e, \mu, \tau$; R_q for $q = b, c$; $A_{FB}(f)$ for $f = \mu, \tau, b, c$; W branching ratios; and $\gamma\gamma$, WW, $WW\gamma$, ZZ, single W, and single Z cross-sections. They are in good agreement with the SM predictions, with the exceptions of R_b (2.1 σ low), $A_{FB}(b)$ (1.6 σ low), and the $W \to \tau\nu_\tau$ branching fraction (2.6 σ high).

The Z boson properties are extracted assuming the SM expressions for the γ–Z interference terms. These have also been tested experimentally by performing more general fits [155,157] to the LEP 1 and LEP 2 data. Assuming family universality this approach introduces three additional parameters relative to the standard fit [10], describing the γ–Z interference contribution to the total hadronic and leptonic cross-sections, $j^{\rm tot}_{\rm had}$ and $j^{\rm tot}_\ell$, and to the leptonic forward-backward asymmetry, $j^{\rm fb}_\ell$. *E.g.*,

$$j^{\rm tot}_{\rm had} \sim g^\ell_V g^{\rm had}_V = 0.277 \pm 0.065, \tag{10.45}$$

which is in agreement with the SM expectation [10] of 0.21 ± 0.01. These are valuable tests of the SM; but it should be cautioned that new physics is not expected to be described by this set of parameters, since (i) they do not account for extra interactions beyond the standard weak neutral current, and (ii) the photonic amplitude remains fixed to its SM value.

Strong constraints on anomalous triple and quartic gauge couplings have been obtained at LEP 2 and the Tevatron as described in the Gauge & Higgs Bosons Particle Listings.

10.4.4. *W and Z decays* :

The partial decay widths for gauge bosons to decay into massless fermions $f_1\overline{f}_2$ (the numerical values include the small EW radiative corrections and final state mass effects) are given by

$$\Gamma(W^+ \to e^+\nu_e) = \frac{G_F M_W^3}{6\sqrt{2}\pi} \approx 226.32 \pm 0.04 \text{ MeV} , \tag{10.46a}$$

$$\Gamma(W^+ \to u_i\overline{d}_j) = \frac{\mathcal{R}_V^q G_F M_W^3}{6\sqrt{2}\pi} |V_{ij}|^2 \approx 705.4 \pm 0.3 \text{ MeV } |V_{ij}|^2, \tag{10.46b}$$

$$\Gamma(Z \to f\bar{f}) = \frac{G_F M_Z^3}{6\sqrt{2}\pi} \left[\mathcal{R}_V^f \bar{g}_V^{f2} + \mathcal{R}_A^f \bar{g}_A^{f2}\right] \approx \begin{cases} 167.15 \pm 0.01 \text{ MeV } (\nu\overline{\nu}), \\ 83.96 \pm 0.01 \text{ MeV } (e^+e^-), \\ 299.91 \pm 0.18 \text{ MeV } (u\overline{u}), \\ 382.78 \pm 0.13 \text{ MeV } (d\overline{d}), \\ 375.76 \mp 0.16 \text{ MeV } (b\overline{b}). \end{cases} \tag{10.46c}$$

Final-state QED and QCD corrections to the vector and axial-vector form factors are given by

$$\mathcal{R}_{V,A}^f = N_C \left[1 + \frac{3}{4}(Q_f^2 \frac{\alpha(s)}{\pi} + \frac{N_C^2 - 1}{2N_C} \frac{\alpha_s(s)}{\pi}) + \cdots\right], \tag{10.47}$$

where $N_C = 3$ (1) is the color factor for quarks (leptons) and the dots indicate finite fermion mass effects proportional to m_f^2/s which are different for $\mathcal{R}_V^f$ and $\mathcal{R}_A^f$, as well as higher-order QCD corrections, which are known to $\mathcal{O}(\alpha_s^4)$ [158–160]. These include singlet contributions starting from two-loop order which are large, strongly top quark mass dependent, family universal, and flavor non-universal [161]. Also the $\mathcal{O}(\alpha^2)$ self-energy corrections from Ref. 162 are taken into account.

For the W decay into quarks, Eq. (10.46*b*), only the universal massless part (non-singlet and $m_q = 0$) of the final-state QCD radiator function in $\mathcal{R}_V$ from Eq. (10.47) is used, and the QED corrections are modified. Expressing the widths in terms of $G_F M_{W,Z}^3$ incorporates the largest radiative corrections from the running QED coupling [52,163]. EW corrections to the Z widths are then taken into account through the effective couplings $\overline{g}_{V,A}^{i2}$. Hence, in the on-shell scheme the Z widths are proportional to $\rho_i \sim 1 + \rho_t$. There is additional (negative) quadratic m_t dependence in the $Z \to b\overline{b}$ vertex corrections [164] which causes $\Gamma(b\overline{b})$ to decrease with m_t. The dominant effect is to multiply $\Gamma(b\overline{b})$ by the vertex correction $1 + \delta\rho_{b\bar{b}}$, where $\delta\rho_{b\bar{b}} \sim 10^{-2}(-\frac{1}{2}m_t^2/M_Z^2 + \frac{1}{5})$. In practice, the corrections are included in $\widehat{\rho}_b$ and $\widehat{\kappa}_b$, as discussed in Sec. 10.4.

For three fermion families the total widths are predicted to be

$$\Gamma_Z \approx 2.4942 \pm 0.0008 \text{ GeV} , \qquad \Gamma_W \approx 2.0895 \pm 0.0006 \text{ GeV} . \tag{10.48}$$

The uncertainties in these predictions are almost entirely induced from the fit error in $\alpha_s(M_Z) = 0.1187 \pm 0.0016$. These predictions are to be compared with the experimental

results, $\Gamma_Z = 2.4952 \pm 0.0023$ GeV [10] and $\Gamma_W = 2.085 \pm 0.042$ GeV (see the Gauge & Higgs Boson Particle Listings for more details).

10.5. Precision flavor physics

In addition to cross-sections, asymmetries, parity violation, W and Z decays, there is a large number of experiments and observables testing the flavor structure of the SM. These are addressed elsewhere in this *Review*, and are generally not included in this Section. However, we identify three precision observables with sensitivity to similar types of new physics as the other processes discussed here. The branching fraction of the flavor changing transition $b \to s\gamma$ is of comparatively low precision, but since it is a loop-level process (in the SM) its sensitivity to new physics (and SM parameters, such as heavy quark masses) is enhanced. A discussion can be found in the 2010 edition of this *Review*. The τ-lepton lifetime and leptonic branching ratios are primarily sensitive to α_s and not affected significantly by many types of new physics. However, having an independent and reliable low energy measurement of α_s in a global analysis allows the comparison with the Z lineshape determination of α_s which shifts easily in the presence of new physics contributions. By far the most precise observable discussed here is the anomalous magnetic moment of the muon (the electron magnetic moment is measured to even greater precision and can be used to determine α, but its new physics sensitivity is suppressed by an additional factor of m_e^2/m_μ^2, unless there is a new light degree of freedom such as a dark Z [165] boson). Its combined experimental and theoretical uncertainty is comparable to typical new physics contributions.

The extraction of α_s from the τ lifetime [166] is standing out from other determinations because of a variety of independent reasons: (i) the τ-scale is low, so that upon extrapolation to the Z scale (where it can be compared to the theoretically clean Z lineshape determinations) the α_s error shrinks by about an order of magnitude; (ii) yet, this scale is high enough that perturbation theory and the operator product expansion (OPE) can be applied; (iii) these observables are fully inclusive and thus free of fragmentation and hadronization effects that would have to be modeled or measured; (iv) duality violation (DV) effects are most problematic near the branch cut but there they are suppressed by a double zero at $s = m_\tau^2$; (v) there are data [37,167] to constrain non-perturbative effects both within and breaking the OPE; (vi) a complete four-loop order QCD calculation is available [160]; (vii) large effects associated with the QCD β-function can be re-summed [168] in what has become known as contour improved perturbation theory (CIPT). However, while there is no doubt that CIPT shows faster convergence in the lower (calculable) orders, doubts have been cast on the method by the observation that at least in a specific model [169], which includes the exactly known coefficients and theoretical constraints on the large-order behavior, ordinary fixed order perturbation theory (FOPT) may nevertheless give a better approximation to the full result. We therefore use the expressions [43,159,160,170],

$$\tau_\tau = \hbar \frac{1 - \mathcal{B}_\tau^s}{\Gamma_\tau^e + \Gamma_\tau^\mu + \Gamma_\tau^{ud}} = 290.75 \pm 0.36 \text{ fs}, \tag{10.49}$$

$$\Gamma_\tau^{ud} = \frac{G_F^2 m_\tau^5 |V_{ud}|^2}{64\pi^3} S(m_\tau, M_Z) \left(1 + \frac{3}{5}\frac{m_\tau^2 - m_\mu^2}{M_W^2}\right) \times$$

$$\left[1 + \frac{\alpha_s(m_\tau)}{\pi} + 5.202\,\frac{\alpha_s^2}{\pi^2} + 26.37\,\frac{\alpha_s^3}{\pi^3} + 127.1\,\frac{\alpha_s^4}{\pi^4} + \frac{\widehat{\alpha}}{\pi}\left(\frac{85}{24} - \frac{\pi^2}{2}\right) + \delta_{\rm NP}\right], \quad (10.50)$$

and Γ_τ^e and Γ_τ^μ can be taken from Eq. (10.6) with obvious replacements. The relative fraction of decays with $\Delta S = -1$, $\mathcal{B}_\tau^s = 0.0292 \pm 0.0004$, is based on experimental data since the value for the strange quark mass, $\widehat{m}_s(m_\tau)$, is not well known and the QCD expansion proportional to $\widehat{m}_s^2$ converges poorly and cannot be trusted. $S(m_\tau, M_Z) = 1.01907 \pm 0.0003$ is a logarithmically enhanced EW correction factor with higher orders re-summed [171]. $\delta_{\rm NP}$ collects non-perturbative and quark-mass suppressed contributions, including the dimension four, six and eight terms in the OPE, as well as DV effects. One group finds the slightly conflicting values $\delta_{\rm NP} = -0.004 \pm 0.012$ [172] and $\delta_{\rm NP} = 0.020 \pm 0.009$ [173], based on OPAL [37] and ALEPH [167] τ spectral functions, respectively. These can be combined to yield the average $\delta_{\rm NP} = 0.0114 \pm 0.0072$. Another analysis [167] obtains $\delta_{\rm NP} = -0.0064 \pm 0.0013$, based largely on the same data sets (see also Ref. 174). We take the arithmetic mean of both groups with an uncertainty that includes both central values, $\delta_{\rm NP} = 0.003 \pm 0.009$. The dominant uncertainty arises from the truncation of the FOPT series and is conservatively taken as the α_s^4 term (this is re-calculated in each call of the fits, leading to an α_s-dependent and thus asymmetric error) until a better understanding of the numerical differences between FOPT and CIPT has been gained. Our perturbative error covers almost the entire range from using CIPT to assuming that the nearly geometric series in Eq. (10.50) continues to higher orders. The experimental uncertainty in Eq. (10.49) is from the combination of the two leptonic branching ratios with the direct τ_τ. Included are also various smaller uncertainties (± 0.15 fs) from other sources. In total we obtain a $\sim 1.6\%$ determination of $\alpha_s^{(5)}(M_Z) = 0.1184^{+0.0020}_{-0.0018}$, which corresponds to $\alpha_s^{(4)}(m_\tau) = 0.323^{+0.018}_{-0.014}$, and updates the result of Refs. 43 and 175. For more details, see Refs. 172 and 173 where the τ spectral functions themselves and an estimate of the unknown α_s^5 term are used as additional inputs.

The world average of the muon anomalous magnetic moment[‡],

$$a_\mu^{\rm exp} = \frac{g_\mu - 2}{2} = (1165920.91 \pm 0.63) \times 10^{-9}, \quad (10.51)$$

[‡] In what follows, we summarize the most important aspects of $g_\mu - 2$, and give some details on the evaluation in our fits. For more details see the dedicated contribution on "The Muon Anomalous Magnetic Moment" in this *Review*. There are some numerical differences, which are well understood and arise because internal consistency of the fits requires the calculation of all observables from analytical expressions and common inputs and fit parameters, so that an independent evaluation is necessary for this Section. Note, that in the spirit of a global analysis based on all available information we have chosen here to consider τ decay data, corrected for isospin breaking effects [21], as well.

is dominated by the final result of the E821 collaboration at BNL [176]. The QED contribution has been calculated to five loops [177] (fully analytic to three loops [178,179] and semi-analytic to four loops [180]) . The estimated SM EW contribution [181–183], $a_\mu^{\rm EW} = (1.54 \pm 0.01) \times 10^{-9}$, which includes two-loop [182] and leading three-loop [183] corrections, is at the level of twice the current uncertainty.

The limiting factor in the interpretation of the result are the uncertainties from hadronic contributions. The most recent evaluations obtained $a_\mu^{\rm had,LO} = (69.31 \pm 0.34) \times 10^{-9}$ [20], $a_\mu^{\rm had,LO} = (68.81 \pm 0.41) \times 10^{-9}$ [184], and $a_\mu^{\rm had,LO} = (69.33 \pm 0.25) \times 10^{-9}$ [35] for the leading-order hadronic effects. These are mainly based on data from $e^+e^- \to$ hadrons, including new data from BaBar and VEPP-2M (see *e.g.* Ref. 20 for a list of references). Our analysis combines the e^+e^- and τ-decay data analysis of Ref. 20 for contributions up to $\sqrt{s} = 2$ GeV, $a_\mu^{\rm had,LO}(2\ {\rm GeV}) = (64.40 \pm 0.30) \times 10^{-9}$, with analytical PQCD expressions [179] beyond 2 GeV. There are promising first results for the determination of $a_\mu^{\rm had,LO}$ from lattice QCD calculations [185], although more work will be needed to reliably control systematic uncertainties to a level comparable with e^+e^- data.

An additional uncertainty is induced by the hadronic three-loop light-by-light scattering contribution. Several recent independent model calculations yield compatible results: $a_\mu^{\rm LBLS}(\alpha^3) = (+1.36 \pm 0.25) \times 10^{-9}$ [186], $a_\mu^{\rm LBLS}(\alpha^3) = +1.37^{+0.15}_{-0.27} \times 10^{-9}$ [187], $a_\mu^{\rm LBLS}(\alpha^3) = (+1.05 \pm 0.26) \times 10^{-9}$ [188], and $a_\mu^{\rm LBLS}(\alpha^3) = (+1.03 \pm 0.29) \times 10^{-9}$ [184]. The sign of this effect is opposite [189] to the one quoted in the 2002 edition of this *Review*, and its magnitude is larger than previous evaluations [189,190]. There is also an upper bound $a_\mu^{\rm LBLS}(\alpha^3) < 1.59 \times 10^{-9}$ [187] but this requires an *ad hoc* assumption, too. Partial results (diagrams with several disconnected quark loops still need to be considered) from lattice simulations are promising, with a moderate (about 25%) statistical uncertainty [191]. Various sources of systematic uncertainties are currently being investigated. For the fits, we take the result from Ref. 184, shifted by 2×10^{-11} to account for the more accurate charm quark treatment of Ref. 187, and with increased error to cover all recent evaluations, resulting in $a_\mu^{\rm LBLS}(\alpha^3) = (+1.05 \pm 0.33) \times 10^{-9}$.

Other hadronic effects at three-loop order [192] and four-loop order [193] contribute $a_\mu^{\rm had,NLO} = (-1.01 \pm 0.01) \times 10^{-9}$ (scaled from and anti-correlated with $a_\mu^{\rm had,LO}$) and $a_\mu^{\rm had,NNLO} = (0.124 \pm 0.001) \times 10^{-9}$, respectively. Correlations with the two-loop hadronic contribution and with $\Delta\alpha(M_Z)$ (see Sec. 10.2) were considered in Ref. 179. The contributions with a hadronic LBLS subgraph have been estimated in Ref. 194, with the result $a_\mu^{\rm LBLS}(\alpha^4) = (0.03 \pm 0.02) \times 10^{-9}$.

Altogether, the SM prediction is

$$a_\mu^{\rm theory} = (1165918.36 \pm 0.44) \times 10^{-9}\ , \tag{10.52}$$

where the error is from the hadronic uncertainties excluding parametric ones such as from α_s and the heavy quark masses. We evaluate the correlation of the total (experimental plus theoretical) uncertainty in a_μ with $\Delta\alpha(M_Z)$ to amount to 22%. The overall 3.3 σ discrepancy between the experimental and theoretical a_μ values could be due to fluctuations (the E821 result is statistics dominated) or underestimates of the theoretical

uncertainties. On the other hand, the deviation could also arise from physics beyond the SM, such as supersymmetric models with large $\tan\beta$ and moderately light superparticle masses [195], or a dark Z boson [165].

10.6. Global fit results

In this section we present the results of global fits to the experimental data discussed in Sec. 10.3–Sec. 10.5. For earlier analyses see Refs. [10,96,196]

Table 10.4: Principal non-Z pole observables, compared with the SM best fit predictions. The first M_W and Γ_W values are from the Tevatron [197,199] and the second ones from LEP 2 [155]. The third M_W is from ATLAS [198]. The value of m_t differs from the one in the Particle Listings since it includes recent preliminary results. The world averages for $g^{\nu e}_{V,A}$ are dominated by the CHARM II [79] results, $g^{\nu e}_V = -0.035 \pm 0.017$ and $g^{\nu e}_A = -0.503 \pm 0.017$. The errors are the total (experimental plus theoretical) uncertainties. The τ_τ value is the τ lifetime world average computed by combining the direct measurements with values derived from the leptonic branching ratios [43]; in this case, the theory uncertainty is included in the SM prediction. In all other SM predictions, the uncertainty is from M_Z, M_H, m_t, m_b, m_c, $\widehat{\alpha}(M_Z)$, and α_s, and their correlations have been accounted for. The column denoted Pull gives the standard deviations.

Quantity	Value	Standard Model	Pull
m_t [GeV]	172.74 ± 0.46	172.96 ± 0.45	-0.5
M_W [GeV]	80.387 ± 0.016	80.358 ± 0.004	1.8
	80.376 ± 0.033		0.6
	80.370 ± 0.019		0.6
Γ_W [GeV]	2.046 ± 0.049	2.089 ± 0.001	-0.9
	2.195 ± 0.083		1.3
M_H [GeV]	125.14 ± 0.15	125.14 ± 0.15	0.0
$g^{\nu e}_V$	-0.040 ± 0.015	-0.0398 ± 0.0001	0.0
$g^{\nu e}_A$	-0.507 ± 0.014	-0.5063	0.0
$Q_W(e)$	-0.0403 ± 0.0053	-0.0476 ± 0.0002	1.4
$Q_W(p)$	0.0719 ± 0.0045	0.0711 ± 0.0002	0.2
$Q_W(\mathrm{Cs})$	-72.62 ± 0.43	-73.23 ± 0.01	1.4
$Q_W(\mathrm{Tl})$	-116.4 ± 3.6	-116.87 ± 0.02	0.1
$\widehat{s}^2_Z$(eDIS)	0.2299 ± 0.0043	0.23122 ± 0.00003	-0.3
τ_τ [fs]	290.75 ± 0.36	290.39 ± 2.17	0.1
$\frac{1}{2}(g_\mu - 2 - \frac{\alpha}{\pi})$	$(4511.18 \pm 0.77) \times 10^{-9}$	$(4508.63 \pm 0.03) \times 10^{-9}$	3.3

The values for m_t [44–47], M_W [155,197,198], Γ_W [155,199], ν-lepton scattering [78–81], the weak charges of the electron [100], the proton [106,107], cesium [110,111] and thallium [112], the weak mixing angle extracted from eDIS [92], the muon anomalous magnetic moment [176], and the τ lifetime are listed in Table 10.4. M_H is our average of the LHC combination from Run 1 [200], $M_H = 125.09 \pm 0.21\,_{\rm stat.} \pm 0.11\,_{\rm syst.}$ GeV, with $M_H = 124.98 \pm 0.19\,_{\rm stat.} \pm 0.21\,_{\rm syst.}$ GeV from ATLAS [201] and $M_H = 125.26 \pm 0.29\,_{\rm stat.} \pm 0.08\,_{\rm syst.}$ GeV from CMS [202] at Run 2, where we conservatively treated the smallest systematic error as common among the three determinations. Likewise, the principal Z pole observables can be found in Table 10.5, where the LEP 1 averages of the ALEPH, DELPHI, L3 and OPAL results include common systematic errors and correlations [10]. The heavy flavor results of LEP 1 and SLD are based on common inputs and correlated, as well [10]. Note that the values of $\Gamma(\ell^+\ell^-)$, Γ(had), and Γ(inv) are not independent of Γ_Z, the R_ℓ, and $\sigma_{\rm had}$ and that the SM errors in those latter are largely dominated by the uncertainty in α_s. Also shown in both tables are the SM predictions for the values of M_Z, M_H, $\alpha_s(M_Z)$, $\Delta\alpha^{(3)}_{\rm had}$ and the heavy quark masses shown in Table 10.6. The predictions result from a global least-square (χ^2) fit to all data using the minimization package MINUIT [203] and the EW library GAPP [22]. In most cases, we treat all input errors (the uncertainties of the values) as Gaussian. The reason is not that we assume that theoretical and systematic errors are intrinsically bell-shaped (which they are not) but because in most cases the input errors are either dominated by the statistical components or they are combinations of many different (including statistical) error sources, which should yield approximately Gaussian *combined* errors by the large number theorem. An exception is the theory dominated error on the τ lifetime, which we recalculate in each χ^2-function call since it depends itself on α_s. Sizes and shapes of the output errors (the uncertainties of the predictions and the SM fit parameters) are fully determined by the fit, and 1 σ errors are defined to correspond to $\Delta\chi^2 = \chi^2 - \chi^2_{\rm min} = 1$, and do not necessarily correspond to the 68.3% probability range or the 39.3% probability contour (for 2 parameters).

The agreement is generally very good. Despite the few discrepancies discussed in the following, the fit describes the data well, with a χ^2/d.o.f. = 47.0/41. The probability of a larger χ^2 is 24%. Only the final result for $g_\mu - 2$ from BNL is currently showing a larger (3.3 σ) conflict. In addition, $A^{(0,b)}_{FB}$ from LEP 1 and A^0_{LR} (SLD) from hadronic final states deviate at the 2 σ level. g^2_L from NuTeV is nominally in conflict with the SM, as well, but the precise status is still unresolved (see Sec. 10.3). We also recall that the values of $\bar{s}^2_\ell$ at CDF and of m_t at DØ are somewhat higher than the determinations from other experiments at hadron colliders, but this is not reflected in the overall χ^2 of the fit because Tevatron combinations are used as inputs.

A_b can be extracted from $A^{(0,b)}_{FB}$ when $A_e = 0.1501 \pm 0.0016$ is taken from a fit to leptonic asymmetries (using lepton universality). The result, $A_b = 0.881 \pm 0.017$, is 3.1 σ below the SM prediction[§] and also 1.6 σ below $A_b = 0.923 \pm 0.020$ obtained from

[§] Alternatively, one can use $A_\ell = 0.1481 \pm 0.0027$, which is from LEP 1 alone and in excellent agreement with the SM, and obtain $A_b = 0.893 \pm 0.022$ which is 1.9 σ low. This

Table 10.5: Principal Z pole observables and their SM predictions (*cf.* Table 10.4). The first $\overline{s}^2_\ell$ is the effective weak mixing angle extracted from the hadronic charge asymmetry, the second is the combined value from the Tevatron [147], and the third from the LHC [152–154]. The values of A_e are (i) from A_{LR} for hadronic final states [140]; (ii) from A_{LR} for leptonic final states and from polarized Bhabba scattering [142]; and (iii) from the angular distribution of the τ polarization at LEP 1. The A_τ values are from SLD and the total τ polarization, respectively.

Quantity	Value	Standard Model	Pull
M_Z [GeV]	91.1876 ± 0.0021	91.1884 ± 0.0020	-0.4
Γ_Z [GeV]	2.4952 ± 0.0023	2.4942 ± 0.0008	0.4
Γ(had) [GeV]	1.7444 ± 0.0020	1.7411 ± 0.0008	—
Γ(inv) [MeV]	499.0 ± 1.5	501.44 ± 0.04	—
$\Gamma(\ell^+\ell^-)$ [MeV]	83.984 ± 0.086	83.959 ± 0.008	—
$\sigma_{\rm had}$[nb]	41.541 ± 0.037	41.481 ± 0.008	1.6
R_e	20.804 ± 0.050	20.737 ± 0.010	1.3
R_μ	20.785 ± 0.033	20.737 ± 0.010	1.4
R_τ	20.764 ± 0.045	20.782 ± 0.010	-0.4
R_b	0.21629 ± 0.00066	0.21582 ± 0.00002	0.7
R_c	0.1721 ± 0.0030	0.17221 ± 0.00003	0.0
$A_{FB}^{(0,e)}$	0.0145 ± 0.0025	0.01618 ± 0.00006	-0.7
$A_{FB}^{(0,\mu)}$	0.0169 ± 0.0013		0.6
$A_{FB}^{(0,\tau)}$	0.0188 ± 0.0017		1.5
$A_{FB}^{(0,b)}$	0.0992 ± 0.0016	0.1030 ± 0.0002	-2.3
$A_{FB}^{(0,c)}$	0.0707 ± 0.0035	0.0735 ± 0.0001	-0.8
$A_{FB}^{(0,s)}$	0.0976 ± 0.0114	0.1031 ± 0.0002	-0.5
$\bar{s}^2_\ell$	0.2324 ± 0.0012	0.23154 ± 0.00003	0.7
	0.23148 ± 0.00033		-0.2
	0.23104 ± 0.00049		-1.0
A_e	0.15138 ± 0.00216	0.1469 ± 0.0003	2.1
	0.1544 ± 0.0060		1.3
	0.1498 ± 0.0049		0.6
A_μ	0.142 ± 0.015		-0.3
A_τ	0.136 ± 0.015		-0.7
	0.1439 ± 0.0043		-0.7
A_b	0.923 ± 0.020	0.9347	-0.6
A_c	0.670 ± 0.027	0.6677 ± 0.0001	0.1
A_s	0.895 ± 0.091	0.9356	-0.4

Table 10.6: Principal SM fit result including mutual correlations (all masses in GeV).

M_Z	91.1884 ± 0.0020	1.00	−0.06	0.00	0.00	0.02	0.03	0.00
$\widehat{m}_t(\widehat{m}_t)$	163.28 ± 0.44	−0.06	1.00	0.00	−0.13	−0.28	0.03	0.00
$\widehat{m}_b(\widehat{m}_b)$	4.180 ± 0.021	0.00	0.00	1.00	0.00	0.00	0.00	0.00
$\widehat{m}_c(\widehat{m}_c)$	1.275 ± 0.009	0.00	−0.13	0.00	1.00	0.45	0.00	0.00
$\alpha_s(M_Z)$	0.1187 ± 0.0016	0.02	−0.28	0.00	0.45	1.00	−0.02	0.00
$\Delta\alpha^{(3)}_{\rm had}(2\ {\rm GeV})$	0.00590 ± 0.00005	0.03	0.03	0.00	0.00	−0.02	1.00	0.00
M_H	125.14 ± 0.15	0.00	0.00	0.00	0.00	0.00	0.00	1.00

$A^{FB}_{LR}(b)$ at SLD. Thus, it appears that at least some of the problem in A_b is due to a statistical fluctuation or other experimental effect in one of the asymmetries. Note, however, that the uncertainty in $A^{(0,b)}_{FB}$ is strongly statistics dominated. The combined value, $A_b = 0.899 \pm 0.013$ deviates by 2.8 σ.

The left-right asymmetry, $A^0_{LR} = 0.15138 \pm 0.00216$ [140], based on all hadronic data from 1992–1998 differs 2.1 σ from the SM expectation of 0.1469 ± 0.0003. The combined value of $A_\ell = 0.1513 \pm 0.0021$ from SLD (using lepton-family universality and including correlations) is also 2.1 σ above the SM prediction; but there is experimental agreement between this SLD value and the LEP 1 value, $A_\ell = 0.1481 \pm 0.0027$, obtained from a fit to $A^{(0,\ell)}_{FB}$, $A_e(\mathcal{P}_\tau)$, and $A_\tau(\mathcal{P}_\tau)$, again assuming universality.

The observables in Table 10.4 and Table 10.5, as well as some other less precise observables, are used in the global fits described below. In all fits, the errors include full statistical, systematic, and theoretical uncertainties. The correlations on the LEP 1 lineshape and τ polarization, the LEP/SLD heavy flavor observables, the SLD lepton asymmetries, and the ν-e scattering observables, are included. The theoretical correlations between $\Delta\alpha^{(5)}_{\rm had}$ and $g_\mu - 2$, and between the W boson mass extractions from ATLAS and the Tevatron, are also accounted for.

The electroweak data allow a simultaneous determination of M_Z, M_H, m_t, and the strong coupling $\alpha_s(M_Z)$. ($\widehat{m}_c$, $\widehat{m}_b$, and $\Delta\alpha^{(3)}_{\rm had}$ are also allowed to float in the fits, subject to the theoretical constraints [19,43] described in Sec. 10.2. These are correlated with α_s.) α_s is determined mainly from R_ℓ, Γ_Z, $\sigma_{\rm had}$, and τ_τ. The global fit to all data, including the hadron collider average $m_t = 172.74 \pm 0.46$ GeV, yields the result in Table 10.6 (the $\overline{\rm MS}$ top quark mass given there corresponds to $m_t = 172.96 \pm 0.45$ GeV). The weak mixing angle, see Table 10.2, is determined to

$$\widehat{s}^2_Z = 0.23122 \pm 0.00003, \qquad s^2_W = 0.22343 \pm 0.00007,$$

while the corresponding effective angle is $\overline{s}^2_\ell = 0.23154 \pm 0.00003$.

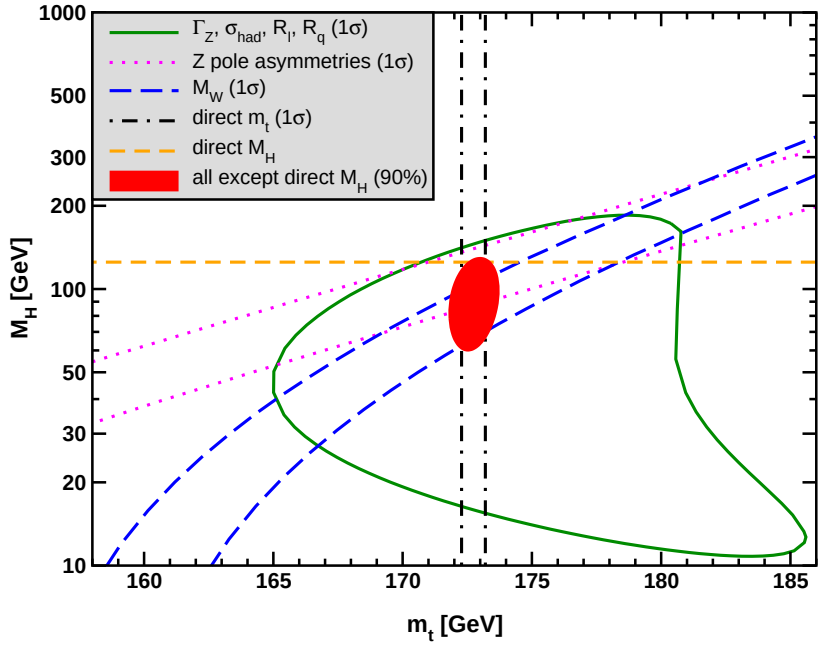

Figure 10.4: Fit result and one-standard-deviation (39.35% for the closed contours and 68% for the others) uncertainties in M_H as a function of m_t for various inputs, and the 90% CL region ($\Delta\chi^2 = 4.605$) allowed by all data. $\alpha_s(M_Z) = 0.1187$ is assumed except for the fits including the Z lineshape. The width of the horizontal dashed (yellow) band is not visible on the scale of the plot.

Removing the kinematic constraint on M_H from LHC gives the loop-level determination from the precision data,

$$M_H = 90^{+17}_{-16}\ \text{GeV}\ , \tag{10.53}$$

which is 1.9 σ below the value in Table 10.4. The latter is also slightly outside the 90% central confidence range,

$$65\ \text{GeV} < M_H < 120\ \text{GeV}\ . \tag{10.54}$$

This is mostly a reflection of the Tevatron determination of M_W, which is 1.8 σ higher than the SM best fit value in Table 10.4. This is illustrated in Fig. 10.4 where one sees that the precision data together with M_H from the LHC prefer that m_t is closer to the upper end of its 1σ allowed range. Conversely, one can remove the direct M_W and Γ_W constraints from the fits and use $M_H = 125.14 \pm 0.15$ GeV to obtain $M_W = 80.355 \pm 0.004$ GeV. This is 2.0 σ below the world average, $M_W = 80.379 \pm 0.012$ GeV.

Finally, one can carry out a fit without including the constraint, $m_t = 172.74 \pm 0.46$ GeV, from the hadron colliders. One obtains $m_t = 176.4 \pm 1.8$ GeV, which is 2.0 σ higher than the direct Tevatron/LHC average. (The indirect prediction is for the $\overline{\text{MS}}$ mass, $\widehat{m}_t(\widehat{m}_t) = 166.5 \pm 1.7$ GeV, which is in the end converted to the pole mass.) The situation is summarized in Fig. 10.5 showing the 1 σ contours in the M_W-m_t plane from the direct and indirect determinations, as well as the combined 90% CL region.

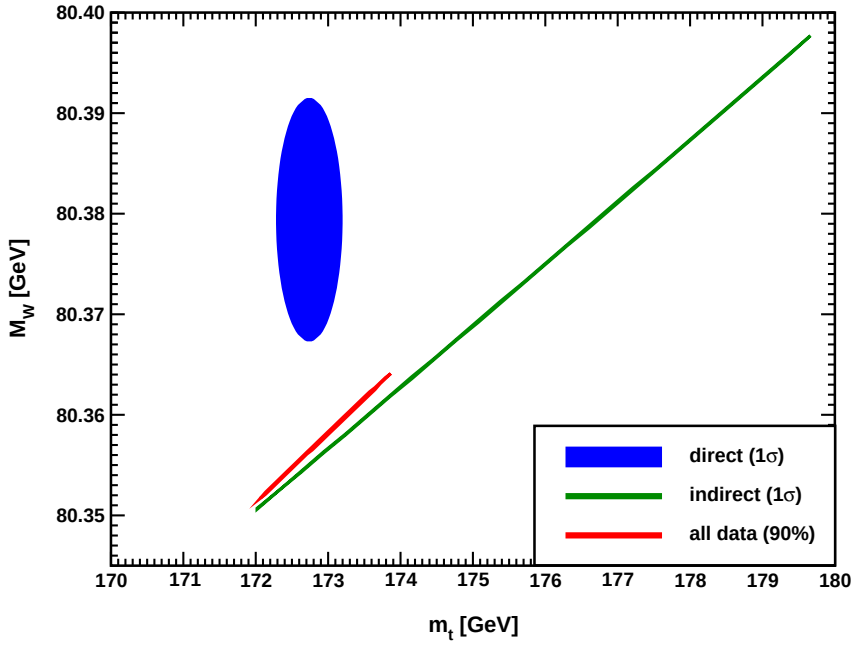

Figure 10.5: One-standard-deviation (39.35%) region in M_W as a function of m_t for the direct and indirect data, and the 90% CL region ($\Delta\chi^2 = 4.605$) allowed by all data.

In view of these tensions it is instructive to study the effect of doubling the uncertainty in $\Delta\alpha^{(3)}_{\rm had}(2\ \text{GeV}) = (58.71 \pm 0.50) \times 10^{-4}$ (see Sec. 10.2) on the loop-level determination of the Higgs boson mass. The result, $M_H = 88^{+18}_{-15}$ GeV, deviates even slightly *more* (2.0 σ) than Eq. (10.53), and demonstrates that the uncertainty in $\Delta\alpha_{\rm had}$ is currently of only secondary importance. Note also that a shift of $\pm 10^{-4}$ in $\Delta\alpha^{(3)}_{\rm had}(2\ \text{GeV})$ corresponds to a shift of ∓ 4.5 GeV in M_H. The hadronic contribution to $\alpha(M_Z)$ is correlated with $g_\mu - 2$ (see Sec. 10.5). The measurement of the latter is higher than the SM prediction, and its inclusion in the fit favors a larger $\alpha(M_Z)$ and a lower M_H from the precision data (currently by 1.7 GeV).

The weak mixing angle can be determined from Z pole observables, M_W, and from a variety of neutral-current processes spanning a very wide Q^2 range. The results (for the older low energy neutral-current data see Refs. 96 and 196, as well as earlier editions of this *Review*) shown in Table 10.7 are in reasonable agreement with each other, indicating the quantitative success of the SM. The largest discrepancy is the value $\widehat{s}^2_Z = 0.23190 \pm 0.00029$ from the forward-backward asymmetries into bottom and charm quarks, which is 2.3 σ above the value 0.23122 ± 0.00003 from the global fit to all data (see Table 10.5). Similarly, $\widehat{s}^2_Z = 0.23064 \pm 0.00028$ from the SLD asymmetries (in both cases when combined with M_Z) is 2.1 σ low.

The extracted Z pole value of $\alpha_s(M_Z)$ is based on a formula with negligible theoretical uncertainty if one assumes the exact validity of the SM. One should keep in mind, however, that this value, $\alpha_s(M_Z) = 0.1203 \pm 0.0028$, is very sensitive to certain types of

Table 10.7: Values of $\widehat{s}^2_Z$, s^2_W, α_s, m_t and M_H [both in GeV] for various data sets. In the fit to the LHC (Tevatron) data the α_s constraint is from the $t\bar{t}$ production [204] (inclusive jet [205]) cross-section.

Data	$\widehat{s}^2_Z$	s^2_W	$\alpha_s(M_Z)$	m_t	M_H
All data	0.23122(3)	0.22332(7)	0.1187(16)	173.0 ± 0.4	125
All data except M_H	0.23107(9)	0.22310(19)	0.1190(16)	172.8 ± 0.5	$90^{+\ 17}_{-\ 16}$
All data except M_Z	0.23113(6)	0.22336(8)	0.1187(16)	172.8 ± 0.5	125
All data except M_W	0.23124(3)	0.22347(7)	0.1191(16)	172.9 ± 0.5	125
All data except m_t	0.23112(6)	0.22304(21)	0.1191(16)	176.4 ± 1.8	125
M_H, M_Z, Γ_Z, m_t	0.23125(7)	0.22351(13)	0.1209(45)	172.7 ± 0.5	125
LHC	0.23110(11)	0.22332(12)	0.1143(24)	172.4 ± 0.5	125
Tevatron + M_Z	0.23102(13)	0.22295(30)	0.1160(45)	174.3 ± 0.7	$100^{+\ 31}_{-\ 26}$
LEP	0.23138(17)	0.22343(47)	0.1221(31)	182 ± 11	274^{+376}_{-152}
SLD + M_Z, Γ_Z, m_t	0.23064(28)	0.22228(54)	0.1182(47)	172.7 ± 0.5	$38^{+\ 30}_{-\ 21}$
$A_{FB}^{(b,c)}$, M_Z, Γ_Z, m_t	0.23190(29)	0.22503(69)	0.1278(50)	172.7 ± 0.5	348^{+187}_{-124}
$M_{W,Z}$, $\Gamma_{W,Z}$, m_t	0.23103(12)	0.22302(25)	0.1192(42)	172.7 ± 0.5	$84^{+\ 22}_{-\ 19}$
low energy + $M_{H,Z}$	0.23176(94)	0.2254(35)	0.1185(19)	156 ± 29	125

new physics such as non-universal vertex corrections. In contrast, the value derived from τ decays, $\alpha_s(M_Z) = 0.1184^{+0.0020}_{-0.0018}$, is theory dominated but less sensitive to new physics. The two values are in reasonable agreement with each other. They are also in good agreement with the averages from jet-event shapes in e^+e^- annihilation (0.1169 ± 0.0034) and lattice simulations (0.1188 ± 0.0011), whereas the DIS average (0.1156 ± 0.0021) is somewhat lower than the Z pole value. For more details, other determinations, and references, see Section 9 on "Quantum Chromodynamics" in this *Review*. In addition, there is a detailed analysis of inclusive cross section measurements for top quark pair production at hadron colliders [206], which yields $\alpha_s = 0.1170^{+0.0034}_{-0.0032}$ after adjustment of the result to correspond to the top quark mass in Eq. (10.9).

Using $\alpha(M_Z)$ and $\widehat{s}^2_Z$ as inputs, one can predict $\alpha_s(M_Z)$ assuming grand unification. One finds [207] $\alpha_s(M_Z) = 0.130 \pm 0.001 \pm 0.01$ for the simplest theories based on the minimal supersymmetric extension of the SM, where the first (second) uncertainty is from the inputs (thresholds). This is slightly larger, but consistent with $\alpha_s(M_Z) = 0.1187 \pm 0.0016$ from our fit, as well as with most other determinations. Non-supersymmetric unified theories predict the low value $\alpha_s(M_Z) = 0.073 \pm 0.001 \pm 0.001$. See also the note on "Supersymmetry" in the Searches Particle Listings.

Table 10.8: Values of the model-independent neutral-current parameters, compared with the SM predictions. There is a second $g^{\nu e}_{LV,LA}$ solution, given approximately by $g^{\nu e}_{LV} \leftrightarrow g^{\nu e}_{LA}$, which is eliminated by e^+e^- data under the assumption that the neutral current is dominated by the exchange of a single Z boson. In the SM predictions, the parametric uncertainties from M_Z, M_H, m_t, m_b, m_c, $\widehat{\alpha}(M_Z)$, and α_s are negligible.

Quantity	Experimental Value	Standard Model	Correlation	
$g^{\nu e}_{LV}$	-0.040 ± 0.015	-0.0398		-0.05
$g^{\nu e}_{LA}$	-0.507 ± 0.014	-0.5063		
$g^{eu}_{AV} + 2\, g^{ed}_{AV}$	0.4914 ± 0.0031	0.4950	-0.88	0.19
$2\, g^{eu}_{AV} - \ g^{ed}_{AV}$	-0.7148 ± 0.0068	-0.7194		-0.22
$2\, g^{eu}_{VA} - \ g^{ed}_{VA}$	-0.13 ± 0.06	-0.0954		
g^{ee}_{VA}	0.0190 ± 0.0027	0.0226		

Most of the parameters relevant to ν-hadron, ν-e, e-hadron, and $e^-e^\pm$ processes are determined uniquely and precisely from the data in "model-independent" fits (*i.e.*, fits which allow for an arbitrary EW gauge theory). The values for the parameters defined in Eqs. (10.15)–(10.18) are given in Table 10.8 along with the predictions of the SM. The agreement is very good. (The ν-hadron results including the original NuTeV data can be found in the 2006 edition of this *Review*, and fits with modified NuTeV constraints in the 2008 and 2010 editions.) The off Z pole e^+e^- results are difficult to present in a model-independent way because Z propagator effects are non-negligible at TRISTAN, PETRA, PEP, and LEP 2 energies. However, assuming e-μ-τ universality, the low energy lepton asymmetries imply [137] $4\,(g^e_A)^2 = 0.99 \pm 0.05$, in good agreement with the SM prediction $\simeq 1$.

10.7. Constraints on new physics

The masses and decay properties of the electroweak bosons and low energy data can be used to search for and set limits on deviations from the SM. We will mainly discuss the effects of exotic particles (with heavy masses $M_{\rm new} \gg M_Z$ in an expansion in $M_Z/M_{\rm new}$) on the gauge boson self-energies. (Brief remarks are made on new physics which is not of this type.) Most of the effects on precision measurements can be described by three gauge self-energy parameters S, T, and U. We will define these, as well as the related parameters ρ_0, ϵ_i, and $\widehat{\epsilon}_i$, to arise from new physics only. In other words, they are equal to zero ($\rho_0 = 1$) exactly in the SM, and do not include any (loop induced) contributions that depend on m_t or M_H, which are treated separately. Our treatment differs from most of the original papers.

The dominant effect of many extensions of the SM can be described by the ρ_0

parameter,

$$\rho_0 \equiv \frac{M_W^2}{M_Z^2\,\widehat{c}^{\,2}_Z\,\widehat{\rho}}\ , \tag{10.55}$$

which describes new sources of SU(2) breaking that cannot be accounted for by the SM Higgs doublet or m_t effects. $\widehat{\rho}$ is calculated as in Eq. (10.12) assuming the validity of the SM. In the presence of $\rho_0 \neq 1$, Eq. (10.55) generalizes the second Eq. (10.12) while the first remains unchanged. Provided that the new physics which yields $\rho_0 \neq 1$ is a small perturbation which does not significantly affect other radiative corrections, ρ_0 can be regarded as a phenomenological parameter which multiplies G_F in Eqs. (10.15)–(10.18), (10.32), and Γ_Z in Eq. (10.46*c*). There are enough data to determine ρ_0, M_H, m_t, and α_s, simultaneously. From the global fit,

$$\rho_0 = 1.00039 \pm 0.00019\ , \tag{10.56}$$

$$\alpha_s(M_Z) = 0.1189 \pm 0.0016\ , \tag{10.57}$$

where as before the uncertainty is from the experimental inputs and does not include the presumably small but difficult to quantify error from unknown higher-order electroweak corrections. The result in Eq. (10.56) is 2.0 σ above the SM expectation, $\rho_0 = 1$. It can be used to constrain higher-dimensional Higgs representations to have vacuum expectation values of less than a few percent of those of the doublets. Indeed, the relation between M_W and M_Z is modified if there are Higgs multiplets with weak isospin $> 1/2$ with significant vacuum expectation values. For a general (charge-conserving) Higgs structure,

$$\rho_0 = \frac{\sum_i [t(i)(t(i)+1) - t_3(i)^2]|v_i|^2}{2\sum_i t_3(i)^2|v_i|^2}, \tag{10.58}$$

where v_i is the expectation value of the neutral component of a Higgs multiplet with weak isospin $t(i)$ and third component $t_3(i)$. In order to calculate to higher orders in such theories one must define a set of four fundamental renormalized parameters which one may conveniently choose to be α, G_F, M_Z, and M_W, since M_W and M_Z are directly measurable. Then $\widehat{s}^{\,2}_Z$ and ρ_0 can be considered dependent parameters.

Eq. (10.56) can also be used to constrain other types of new physics. For example, non-degenerate multiplets of heavy fermions or scalars break the vector part of weak SU(2) and lead to a decrease in the value of M_Z/M_W. Each non-degenerate SU(2) doublet $\binom{f_1}{f_2}$ yields a positive contribution to ρ_0 [208] of

$$\frac{C\,G_F}{8\sqrt{2}\pi^2}\Delta m^2, \tag{10.59}$$

where

$$\Delta m^2 \equiv m_1^2 + m_2^2 - \frac{4m_1^2 m_2^2}{m_1^2 - m_2^2}\ln\frac{m_1}{m_2} \geq (m_1 - m_2)^2, \tag{10.60}$$

and $C = 1$ (3) for color singlets (triplets). Eq. (10.56) taken together with Eq. (10.59) implies the following constraint on the mass splitting at the 90% CL,

$$(16\ \text{GeV})^2 < \sum_i \frac{C_i}{3}\,\Delta m_i^2 < (48\ \text{GeV})^2, \tag{10.61}$$

where the sum runs over all new-physics doublets, for example fourth-family quarks or leptons, $\binom{t'}{b'}$ or $\binom{\nu'}{\ell'-}$, vector-like fermion doublets (which contribute to the sum in Eq. (10.61) with an extra factor of 2), and scalar doublets such as $\binom{\tilde{t}}{\tilde{b}}$ in Supersymmetry (in the absence of L–R mixing).

Non-degenerate multiplets usually imply $\rho_0 > 1$. Similarly, heavy Z' bosons decrease the prediction for M_Z due to mixing and generally lead to $\rho_0 > 1$ [209]. On the other hand, additional Higgs doublets which participate in spontaneous symmetry breaking [210] or heavy lepton doublets involving Majorana neutrinos [211], both of which have more complicated expressions, as well as the vacuum expectation values of Higgs triplets or higher-dimensional representations can contribute to ρ_0 with either sign. Allowing for the presence of heavy degenerate chiral multiplets (the S parameter, to be discussed below) affects the determination of ρ_0 from the data, at present leading to a larger value.

A number of authors [212–217] have considered the general effects on neutral-current and Z and W boson observables of various types of heavy (*i.e.*, $M_{\rm new} \gg M_Z$) physics which contribute to the W and Z self-energies but which do not have any direct coupling to the ordinary fermions. In addition to non-degenerate multiplets, which break the vector part of weak SU(2), these include heavy degenerate multiplets of chiral fermions which break the axial generators.

Such effects can be described by just three parameters, S, T, and U, at the (EW) one-loop level. (Three additional parameters are needed if the new physics scale is comparable to M_Z [218]. Further generalizations, including effects relevant to LEP 2, are described in Ref. 219.) T is proportional to the difference between the W and Z self-energies at $Q^2 = 0$ (*i.e.*, vector SU(2)-breaking), while S ($S + U$) is associated with the difference between the Z (W) self-energy at $Q^2 = M_{Z,W}^2$ and $Q^2 = 0$ (axial SU(2)-breaking). Denoting the contributions of new physics to the various self-energies by $\Pi_{ij}^{\rm new}$, we have

$$\widehat{\alpha}(M_Z)T \equiv \frac{\Pi_{WW}^{\rm new}(0)}{M_W^2} - \frac{\Pi_{ZZ}^{\rm new}(0)}{M_Z^2}\ , \tag{10.62a}$$

$$\begin{aligned}\frac{\widehat{\alpha}(M_Z)}{4\,\widehat{s}_Z^2\widehat{c}_Z^2}S \equiv{}& \frac{\Pi_{ZZ}^{\rm new}(M_Z^2) - \Pi_{ZZ}^{\rm new}(0)}{M_Z^2} - \\ & \frac{\widehat{c}_Z^2 - \widehat{s}_Z^2}{\widehat{c}_Z\widehat{s}_Z}\,\frac{\Pi_{Z\gamma}^{\rm new}(M_Z^2)}{M_Z^2} - \frac{\Pi_{\gamma\gamma}^{\rm new}(M_Z^2)}{M_Z^2}\ ,\end{aligned} \tag{10.62b}$$

$$\frac{\widehat{\alpha}(M_Z)}{4\,\widehat{s}_Z^2}\,(S+U) \equiv \frac{\Pi_{WW}^{\rm new}(M_W^2) - \Pi_{WW}^{\rm new}(0)}{M_W^2} -$$

$$\frac{\widehat{c}_Z}{\widehat{s}_Z}\,\frac{\Pi^{\rm new}_{Z\gamma}(M_Z^2)}{M_Z^2} - \frac{\Pi^{\rm new}_{\gamma\gamma}(M_Z^2)}{M_Z^2}\ . \qquad (10.62c)$$

S, T, and U are defined with a factor proportional to $\widehat{\alpha}$ removed, so that they are expected to be of order unity in the presence of new physics. In the $\overline{\rm MS}$ scheme as defined in Ref. 53, the last two terms in Eqs. (10.62b) and (10.62c) can be omitted (as was done in some earlier editions of this *Review*). These three parameters are related to other parameters (S_i, h_i, $\widehat{\epsilon}_i$) defined in Refs. [53,213,214] by

$$\begin{aligned} T &= h_V = \widehat{\epsilon}_1/\widehat{\alpha}(M_Z), \\ S &= h_{AZ} = S_Z = 4\,\widehat{s}^2_Z\,\widehat{\epsilon}_3/\widehat{\alpha}(M_Z), \\ U &= h_{AW} - h_{AZ} = S_W - S_Z = -4\,\widehat{s}^2_Z\,\widehat{\epsilon}_2/\widehat{\alpha}(M_Z). \end{aligned} \qquad (10.63)$$

A heavy non-degenerate multiplet of fermions or scalars contributes positively to Tas

$$\rho_0 - 1 = \frac{1}{1-\widehat{\alpha}(M_Z)T} - 1 \simeq \widehat{\alpha}(M_Z)T, \qquad (10.64)$$

where $\rho_0 - 1$ is given in Eq. (10.59). The effects of non-standard Higgs representations cannot be separated from heavy non-degenerate multiplets unless the new physics has other consequences, such as vertex corrections. Most of the original papers defined T to include the effects of loops only. However, we will redefine T to include all new sources of SU(2) breaking, including non-standard Higgs, so that T and ρ_0 are equivalent by Eq. (10.64).

A multiplet of heavy degenerate chiral fermions yields

$$S = \frac{C}{3\pi}\sum_i \Big(t_{3L}(i) - t_{3R}(i)\Big)^2, \qquad (10.65)$$

where $t_{3L,R}(i)$ is the third component of weak isospin of the left-(right-)handed component of fermion i and C is the number of colors. For example, a heavy degenerate ordinary or mirror family would contribute $2/3\pi$ to S. In models with warped extra dimensions, sizeable correction to the S parameter are generated by mixing effects between the SM gauge bosons and their Kaluza-Klein (KK) excitations. One finds $S \approx 30v^2/M^2_{KK}$, where M_{KK} is the mass of the KK gauge bosons [220]. Large positive values $S > 0$ can also be generated in models with dynamical electroweak symmetry breaking, where the Higgs boson is composite. In simple composite Higgs models, the dominant contribution stems from heavy spin-1 resonances of the strong dynamics, leading to $S \approx 4\pi v^2(M_V^{-2} + M_A^{-2})$, where $M_{V,A}$ are the masses of the lightest vector and axial-vector resonances, respectively [221].

On the other hand, negative values $S < 0$ are possible, for example, for models of walking Technicolor [222] or loops involving scalars or Majorana particles [223]. The simplest origin of $S < 0$ would probably be an additional heavy Z' boson [209].

Supersymmetric extensions of the SM generally give very small effects. See Refs. 224 and 225 and the note on "Supersymmetry" in the Searches Particle Listings for a complete set of references.

Most simple types of new physics yield $U = 0$, although there are counter-examples, such as the effects of anomalous triple gauge vertices [214].

The SM expressions for observables are replaced by

$$M_Z^2 = M_{Z0}^2 \, \frac{1 - \widehat{\alpha}(M_Z)T}{1 - G_F M_{Z0}^2 S/2\sqrt{2}\pi} \ ,$$

$$M_W^2 = M_{W0}^2 \, \frac{1}{1 - G_F M_{W0}^2 (S+U)/2\sqrt{2}\pi} \ , \tag{10.66}$$

where M_{Z0} and M_{W0} are the SM expressions (as functions of m_t and M_H) in the $\overline{\rm MS}$ scheme. Furthermore,

$$\Gamma_Z = \frac{M_Z^3 \beta_Z}{1 - \widehat{\alpha}(M_Z)T} \ , \qquad \Gamma_W = M_W^3 \beta_W \ , \qquad A_i = \frac{A_{i0}}{1 - \widehat{\alpha}(M_Z)T} \ , \tag{10.67}$$

where β_Z and β_W are the SM expressions for the reduced widths Γ_{Z0}/M_{Z0}^3 and Γ_{W0}/M_{W0}^3, M_Z and M_W are the physical masses, and A_i (A_{i0}) is a neutral-current amplitude (in the SM).

The data allow a simultaneous determination of $\widehat{s}^2_Z$ (from the Z pole asymmetries), S (from M_Z), U (from M_W), T (mainly from Γ_Z), α_s (from R_ℓ, $\sigma_{\rm had}$, and τ_τ), M_H and m_t (from the hadron colliders), with little correlation among the SM parameters:

$$\begin{aligned} S &= 0.02 \pm 0.10 \ , \\ T &= 0.07 \pm 0.12 \ , \\ U &= 0.00 \pm 0.09 \ , \end{aligned} \tag{10.68}$$

$\widehat{s}^2_Z = 0.23113 \pm 0.00014$, and $\alpha_s(M_Z) = 0.1189 \pm 0.0016$, where the uncertainties are from the inputs. The parameters in Eqs. (10.68), which by definition are due to new physics only, are in excellent agreement with the SM values of zero. Fixing $U = 0$, which is motivated by the fact that U is suppressed by an additional factor $M_{\rm new}^2/M_Z^2$ compared to S and T [226], greatly improves the precision on S and particularly T,

$$\begin{aligned} S &= 0.02 \pm 0.07 \ , \\ T &= 0.06 \pm 0.06 \ , \end{aligned} \tag{10.69}$$

see Fig. 10.6. Using Eq. (10.64), the value of ρ_0 corresponding to T in Eq. (10.68) is 1.0005 ± 0.0009, while the one corresponding to Eq. (10.69) is 1.0005 ± 0.0005. Thus, the multi-parameter fits are consistent with $\rho_0 = 1$, in contrast to the fit with $S = U = 0$ in Eq. (10.56). There is a strong correlation (92%) between the S and T parameters. The

U parameter is -66% (-86%) anti-correlated with S (T). The allowed regions in S–T are shown in Fig. 10.6. From Eqs. (10.68) one obtains $S < 0.18$ and $T < 0.26$ at 95% CL, where the former puts the constraint $M_{KK} \gtrsim 3.2$ TeV on the masses of KK gauge bosons in warped extra dimensions. In minimal composite Higgs models, the bound on S requires $M_V \gtrsim 4$ TeV [227], but this constraint can be relaxed, *e.g.*, if the fermionic sector is also allowed to be partially composite [228,229].

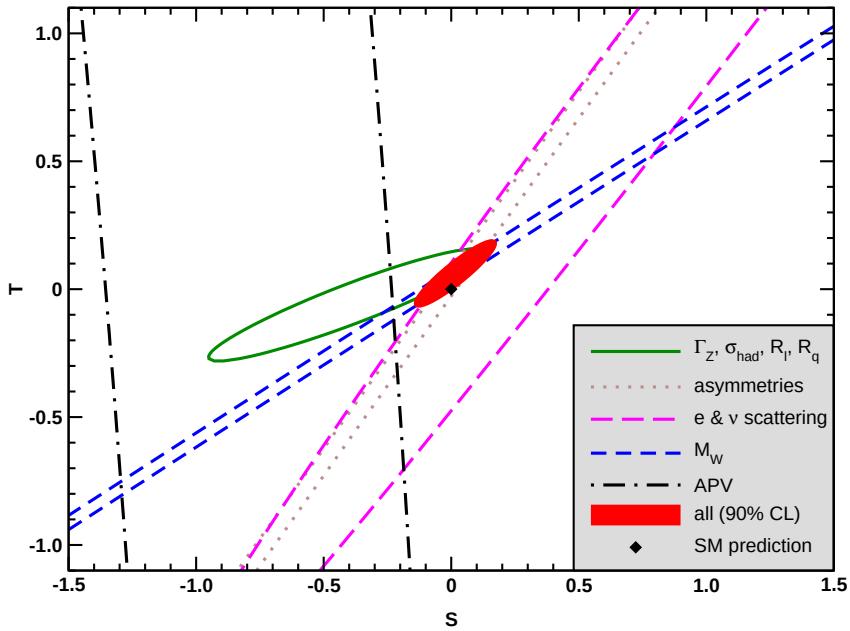

Figure 10.6: 1 σ constraints (39.35% for the closed contours and 68% for the others) on S and T (for $U = 0$) from various inputs combined with M_Z. S and T represent the contributions of new physics only. Data sets not involving M_W or Γ_W are insensitive to U. With the exception of the fit to all data, we fix $\alpha_s = 0.1187$. The black dot indicates the Standard Model values $S = T = 0$.

The S parameter can also be used to constrain the number of fermion families, *under the assumption* that there are no new contributions to T or U and therefore that any new families are degenerate; then an extra generation of SM fermions is excluded at the 9 σ level corresponding to $N_F = 2.75 \pm 0.14$. This can be compared to the fit to the number of light neutrinos given in Eq. (10.37), $N_\nu = 2.991 \pm 0.007$. However, the S parameter fits are valid even for a very heavy fourth family neutrino. Allowing T to vary as well, the constraint on a fourth family is weaker [230]. However, a heavy fourth family would increase the Higgs production cross-section through gluon fusion by a factor ~ 9, which is in considerable tension with the observed Higgs signal at LHC. Combining the limits from electroweak precision data with the measured Higgs production rate and limits from direct searches for heavy quarks [231], a fourth family of chiral fermions is now excluded by more than five standard deviations [232]. Similar remarks apply to a

heavy mirror family [233] involving right-handed SU(2) doublets and left-handed singlets. In contrast, new doublets that receive most of their mass from a different source than the Higgs vacuum expectation value, such as vector-like fermion doublets or scalar doublets in Supersymmetry, give small or no contribution to S, T, U and the Higgs production cross-section and thus are still allowed. Partial or complete vector-like fermion families are predicted in many grand unified theories [234].

As discussed in Sec. 10.6, there is a 4.0% deviation in the asymmetry parameter A_b. Assuming that this is due to new physics affecting preferentially the third generation, we can perform a fit allowing additional $Z \to b\bar{b}$ vertex corrections ρ_b and κ_b as in Eq. (10.33) (here defined to be due to new physics only with the SM contributions removed), as well as S, T, U, and the SM parameters, with the result,

$$\rho_b = 0.059 \pm 0.020 \ , \qquad\qquad \kappa_b = 0.196 \pm 0.067 \ , \tag{10.70}$$

with an almost perfect correlation of 99% (because R_b is much better determined than A_b). The central values of the oblique parameters are close to their SM values of zero, and there is little change in the SM parameters. Given that a $\sim 20\%$ correction to κ_b would be necessary, it would be difficult to account for the deviation in A_b by new physics that enters only at the level of radiative corrections. Thus, if it is due to new physics, it is most likely of tree-level type affecting preferentially the third generation. Examples include the decay of a scalar neutrino resonance [235], mixing of the b quark with heavy exotics [236], and a heavy Z' with family non-universal couplings [237,238]. It is difficult, however, to simultaneously account for R_b without tuning, which has been measured on the Z peak and off-peak [239] at LEP 1. An average of R_b measurements at LEP 2 at energies between 133 and 207 GeV is 2.1 σ below the SM prediction, while $A_{FB}^{(b)}$ (LEP 2) is 1.6 σ low [156].

There is no simple parametrization to describe the effects of every type of new physics on every possible observable. The S, T, and U formalism describes many types of heavy physics which affect only the gauge self-energies, and it can be applied to all precision observables. However, new physics which couples directly to ordinary fermions cannot be fully parametrized in the S, T, and U framework. Examples include heavy Z' bosons [209], mixing with exotic fermions [240], leptoquark exchange [155,241], supersymmetric models [225], strong EW dynamics [228], Little Higgs models [242], and TeV-scale extra spatial dimensions [243]. These types of new physics can be parametrized in a model-indepdendent way by using an effective field theory description. Here the SM is extended by a set of higher-dimensional operators, denoted $\mathcal{O}_i$,

$$\mathcal{L} = \mathcal{L}_{\rm SM} + \sum_{d>4} \sum_i \frac{C_i}{\Lambda^{d-4}} \mathcal{O}_i \ , \tag{10.71}$$

where Λ is the characteristic scale of the new physics sector, which is assumed to satisfy $\Lambda \gg v$. For EW precision observables, the leading new operators enter at dimension $d = 6$. With current data on M_W and Z-pole observables, Λ is constrained to be larger than $\mathcal{O}$(TeV) if the Wilson coefficients C_i are of order 1 [244].

An alternate formalism [245] defines parameters, ϵ_1, ϵ_2, ϵ_3, and ϵ_b in terms of the specific observables M_W/M_Z, $\Gamma_{\ell\ell}$, $A_{FB}^{(0,\ell)}$, and R_b. The definitions coincide with those for $\widehat{\epsilon}_i$ in Eqs. (10.62) and (10.63) for physics which affects gauge self-energies only, but the ϵ's now parametrize arbitrary types of new physics. However, the ϵ's are not related to other observables unless additional model-dependent assumptions are made.

Limits on new four-Fermi operators and on leptoquarks using LEP 2 and lower energy data are given in Refs. 155 and 246. Constraints on various types of new physics are reviewed in Refs. [7,96,123,139,247,248]. For a particularly well motivated and explored type of physics beyond the SM, see the note on "The Z' Searches" in the Gauge & Higgs Boson Particle Listings.

Acknowledgments:

It is a pleasure to thank Rodolfo Ferro-Hernández for discussions, for performing some of the calculations and checks, and for producing the plot in Fig. 10.2. J.E. is supported by CONACyT (Mexico) project 252167–F and the German–Mexican research collaboration grant SP 778/4–1 (DFG) and 278017 (CONACyT). A.F. is supported in part by the National Science Foundation under grant no. PHY–1519175.

References:

1. S.L. Glashow, Nucl. Phys. **22**, 579 (1961);
   S. Weinberg, Phys. Rev. Lett. **19**, 1264 (1967);
   A. Salam, p. 367 of *Elementary Particle Theory*, ed. N. Svartholm (Almquist and Wiksells, Stockholm, 1969);
   S.L. Glashow, J. Iliopoulos, and L. Maiani, Phys. Rev. **D2**, 1285 (1970).
2. CKMfitter Group: J. Charles *et al.*, Eur. Phys. J. **C41**, 1 (2005); updated results and plots are available at `http://ckmfitter.in2p3.fr`.
3. For reviews, see the Section on "Status of Higgs Boson Physics" in this *Review*;
   J. Gunion *et al.*, *The Higgs Hunter's Guide*, (Addison-Wesley, Redwood City, 1990);
   M. Carena and H.E. Haber, Prog. in Part. Nucl. Phys. **50**, 63 (2003);
   A. Djouadi, Phys. Reports **457**, 1 (2008).
4. For reviews, see E.D. Commins and P.H. Bucksbaum, *Weak Interactions of Leptons and Quarks*, (Cambridge Univ. Press, 1983);
   G. Barbiellini and C. Santoni, Riv. Nuovo Cimento **9(2)**, 1 (1986);
   N. Severijns, M. Beck, and O. Naviliat-Cuncic, Rev. Mod. Phys. **78**, 991 (2006);
   W. Fetscher and H.J. Gerber, p. 657 of Ref. 5;
   J. Deutsch and P. Quin, p. 706 of Ref. 5;
   P. Herczeg, p. 786 of Ref. 5;
   P. Herczeg, Prog. in Part. Nucl. Phys. **46**, 413 (2001).
5. *Precision Tests of the Standard Electroweak Model*, ed. P. Langacker (World Scientific, Singapore, 1995).
6. J. Erler and M.J. Ramsey-Musolf, Prog. in Part. Nucl. Phys. **54**, 351 (2005).
7. P. Langacker, *The Standard Model and Beyond*, (CRC Press, New York, 2009).
8. T. Kinoshita, *Quantum Electrodynamics*, (World Scientific, Singapore, 1990).
9. S.G. Karshenboim, Phys. Reports **422**, 1 (2005).

10. ALEPH, DELPHI, L3, OPAL, SLD, LEP Electroweak Working Group, SLD Electroweak and Heavy Flavour Groups: S. Schael *et al.*, Phys. Reports **427**, 257 (2006); for updates see `http://lepewwg.web.cern.ch/LEPEWWG/`.
11. MuLan: D.M. Webber *et al.*, Phys. Rev. Lett. **106**, 041803 (2011).
12. T. Kinoshita and A. Sirlin, Phys. Rev. **113**, 1652 (1959).
13. T. van Ritbergen and R.G. Stuart, Nucl. Phys. **B564**, 343 (2000); M. Steinhauser and T. Seidensticker, Phys. Lett. **B467**, 271 (1999).
14. Y. Nir, Phys. Lett. **B221**, 184 (1989).
15. A. Pak and A. Czarnecki, Phys. Rev. Lett. **100**, 241807 (2008).
16. P.J. Mohr, B.N. Taylor, and D.B. Newell, `arXiv:1507.07956 [physics.atom-ph]`.
17. For a review, see S. Mele, `arXiv:hep-ex/0610037`.
18. S. Fanchiotti, B. Kniehl, and A. Sirlin, Phys. Rev. **D48**, 307 (1993) and references thereinma.
19. J. Erler, Phys. Rev. **D59**, 054008 (1999).
20. M. Davier *et al.*, Eur. Phys. J. **C77**, 827 (2017).
21. F. Jegerlehner and R. Szafron, Eur. Phys. J. **C71**, 1632 (2011); the quoted value uses additional information thankfully provided to us by the author in a private communication.
22. J. Erler, `hep-ph/0005084`.
23. M. Steinhauser, Phys. Lett. **B429**, 158 (1998).
24. K.G. Chetyrkin, J.H. Kühn, and M. Steinhauser, Nucl. Phys. **B482**, 213 (1996).
25. B.V. Geshkenbein and V.L. Morgunov, Phys. Lett. **B352**, 456 (1995).
26. M.L. Swartz, Phys. Rev. **D53**, 5268 (1996).
27. N.V. Krasnikov and R. Rodenberg, Nuovo Cimento **111A**, 217 (1998).
28. J.H. Kühn and M. Steinhauser, Phys. Lett. **B437**, 425 (1998).
29. S. Groote *et al.*, Phys. Lett. **B440**, 375 (1998).
30. A.D. Martin, J. Outhwaite, and M.G. Ryskin, Phys. Lett. **B492**, 69 (2000).
31. J.F. de Troconiz and F.J. Yndurain, Phys. Rev. **D65**, 093002 (2002).
32. H. Burkhardt and B. Pietrzyk, Phys. Rev. **D84**, 037502 (2011).
33. K. Hagiwara *et al.*, J. Phys. **G38**, 085003 (2011).
34. F. Jegerlehner, `arXiv:1711.06089 [hep-ph]`.
35. A. Keshavarzi, D. Nomura and T. Teubner, `arXiv:1802.02995 [hep-ph]`.
36. M. Davier *et al.*, Eur. Phys. J. **C71**, 1515 (2011).
37. OPAL: K. Ackerstaff *et al.*, Eur. Phys. J. **C7**, 571 (1999).
38. CLEO: S. Anderson *et al.*, Phys. Rev. **D61**, 112002 (2000).
39. ALEPH: S. Schael *et al.*, Phys. Reports **421**, 191 (2005).
40. Belle: M. Fujikawa *et al.*: Phys. Rev. **D78**, 072006 (2008).
41. J. Erler, Eur. Phys. J. **C77**, 99 (2017).
42. V.A. Novikov *et al.*, Phys. Reports **41**, 1 (1978).
43. J. Erler and M. Luo, Phys. Lett. **B558**, 125 (2003).
44. Tevatron Electroweak Working Group for the CDF and DØ Collaborations: `arXiv:1608.01881 [hep-ex]`.
45. ATLAS: `cds.cern.ch/record/2285809/files/ATLAS-CONF-2017-071.pdf`.
46. CMS: `cds.cern.ch/record/2235162/files/TOP-15-012-pas.pdf`.

47. CMS: cds.cern.ch/record/2284594/files/TOP-17-007-pas.pdf.
48. M. Beneke *et al.*, Phys. Lett. **B775**, 63 (2017).
49. P. Marquard *et al.*, Phys. Rev. Lett. **114**, 142002 (2015).
50. M. Butenschoen *et al.*, Phys. Rev. Lett. **117**, 232001 (2016);
A. Andreassen, M.D. Schwartz, JHEP **1710**, 151 (2017).
51. DØ: V.M. Abazov *et al.*, Phys. Rev. Lett. **113**, 032002 (2014).
52. A. Sirlin, Phys. Rev. **D22**, 971 (1980);
D.C. Kennedy *et al.*, Nucl. Phys. **B321**, 83 (1989);
D.Yu. Bardin *et al.*, Z. Phys. **C44**, 493 (1989);
W. Hollik, Fortsch. Phys. **38**, 165 (1990);
for reviews, see W. Hollik, pp. 37 and 117, and W. Marciano, p. 170 of Ref. 5.
53. W.J. Marciano and J.L. Rosner, Phys. Rev. Lett. **65**, 2963 (1990).
54. G. Degrassi, S. Fanchiotti, and A. Sirlin, Nucl. Phys. **B351**, 49 (1991).
55. K.S. Kumar *et al.*, Ann. Rev. Nucl. and Part. Sci. **63**, 237 (2013).
56. G. Degrassi and A. Sirlin, Nucl. Phys. **B352**, 342 (1991);
P. Gambino and A. Sirlin, Phys. Rev. **D49**, 1160 (1994).
57. ZFITTER: A.B. Arbuzov *et al.*, Comput. Phys. Commun. **174**, 728 (2006) and references therein.
58. R. Barbieri *et al.*, Nucl. Phys. **B409**, 105 (1993);
J. Fleischer, O.V. Tarasov, and F. Jegerlehner, Phys. Lett. **B319**, 249 (1993).
59. G. Degrassi, P. Gambino, and A. Vicini, Phys. Lett. **B383**, 219 (1996);
G. Degrassi, P. Gambino, and A. Sirlin, Phys. Lett. **B394**, 188 (1997).
60. A. Freitas *et al.*, Phys. Lett. **B495**, 338 (2000) and *ibid.* **570**, 260(E) (2003);
M. Awramik and M. Czakon, Phys. Lett. **B568**, 48 (2003).
61. A. Freitas *et al.*, Nucl. Phys. **B632**, 189 (2002) and *ibid.* **666**, 305(E) (2003);
M. Awramik and M. Czakon, Phys. Rev. Lett. **89**, 241801 (2002);
A. Onishchenko and O. Veretin, Phys. Lett. **B551**, 111 (2003).
62. M. Awramik *et al.*, Phys. Rev. Lett. **93**, 201805 (2004);
W. Hollik, U. Meier, and S. Uccirati, Nucl. Phys. **B731**, 213 (2005).
63. M. Awramik, M. Czakon, and A. Freitas, Phys. Lett. **B642**, 563 (2006);
W. Hollik, U. Meier, and S. Uccirati, Nucl. Phys. **B765**, 154 (2007).
64. G. Degrassi, P. Gambino and P.P. Giardino, JHEP **1505**, 154 (2015).
65. M. Awramik *et al.*, Phys. Rev. **D69**, 053006 (2004).
66. A. Djouadi and C. Verzegnassi, Phys. Lett. **B195**, 265 (1987);
A. Djouadi, Nuovo Cimento **100A**, 357 (1988).
67. K.G. Chetyrkin, J.H. Kühn, and M. Steinhauser, Phys. Lett. **B351**, 331 (1995).
68. Y. Schröder and M. Steinhauser, Phys. Lett. **B622**, 124 (2005);
K.G. Chetyrkin *et al.*, Phys. Rev. Lett. **97**, 102003 (2006);
R. Boughezal and M. Czakon, Nucl. Phys. **B755**, 221 (2006);
L. Avdeev *et al.*, Phys. Lett. **B336**, 560 (1994) and *ibid.* **B349**, 597(E) (1995).
69. B.A. Kniehl, J.H. Kühn, and R.G. Stuart, Phys. Lett. **B214**, 621 (1988);
B.A. Kniehl, Nucl. Phys. **B347**, 86 (1990);
F. Halzen and B.A. Kniehl, Nucl. Phys. **B353**, 567 (1991);

A. Djouadi and P. Gambino, Phys. Rev. **D49**, 3499 (1994) and *ibid.* **53**, 4111(E) (1996).
70. A. Anselm, N. Dombey, and E. Leader, Phys. Lett. **B312**, 232 (1993).
71. K.G. Chetyrkin, J.H. Kühn, and M. Steinhauser, Phys. Rev. Lett. **75**, 3394 (1995).
72. J.J. van der Bij *et al.*, Phys. Lett. **B498**, 156 (2001);
M. Faisst *et al.*, Nucl. Phys. **B665**, 649 (2003).
73. R. Boughezal, J.B. Tausk, and J.J. van der Bij, Nucl. Phys. **B725**, 3 (2005).
74. M. Awramik, M. Czakon, and A. Freitas, JHEP **0611**, 048 (2006).
75. J. Erler and S. Su, Prog. in Part. Nucl. Phys. **71**, 119 (2013).
76. J.M. Conrad, M.H. Shaevitz, and T. Bolton, Rev. Mod. Phys. **70**, 1341 (1998).
77. Z. Berezhiani and A. Rossi, Phys. Lett. **B535**, 207 (2002);
S. Davidson *et al.*, JHEP **0303**, 011 (2003);
A. Friedland, C. Lunardini and C. Pena-Garay, Phys. Lett. **B594**, 347 (2004).
78. J. Panman, p. 504 of Ref. 5;
CHARM: J. Dorenbosch *et al.*, Z. Phys. **C41**, 567 (1989);
CALO: L.A. Ahrens *et al.*, Phys. Rev. **D41**, 3297 (1990).
79. CHARM II: P. Vilain *et al.*, Phys. Lett. **B335**, 246 (1994).
80. ILM: R.C. Allen *et al.*, Phys. Rev. **D47**, 11 (1993);
LSND: L.B. Auerbach *et al.*, Phys. Rev. **D63**, 112001 (2001).
81. TEXONO: M. Deniz *et al.*, Phys. Rev. **D81**, 072001 (2010).
82. For reviews, see G.L. Fogli and D. Haidt, Z. Phys. **C40**, 379 (1988);
F. Perrier, p. 385 of Ref. 5.
83. CDHS: A. Blondel *et al.*, Z. Phys. **C45**, 361 (1990).
84. CHARM: J.V. Allaby *et al.*, Z. Phys. **C36**, 611 (1987).
85. CCFR: K.S. McFarland *et al.*, Eur. Phys. J. **C1**, 509 (1998).
86. R.M. Barnett, Phys. Rev. **D14**, 70 (1976);
H. Georgi and H.D. Politzer, Phys. Rev. **D14**, 1829 (1976).
87. LAB-E: S.A. Rabinowitz *et al.*, Phys. Rev. Lett. **70**, 134 (1993).
88. E.A. Paschos and L. Wolfenstein, Phys. Rev. **D7**, 91 (1973).
89. NuTeV: G.P. Zeller *et al.*, Phys. Rev. Lett. **88**, 091802 (2002).
90. J. Erler *et al.*, Ann. Rev. Nucl. and Part. Sci. **64**, 269 (2014).
91. SSF: C.Y. Prescott *et al.*, Phys. Lett. **B84**, 524 (1979).
92. JLab-PVDIS: D. Wang *et al.*, Nature **506**, 67 (2014) and Phys. Rev. **C91**, 045506 (2015).
93. E.J. Beise, M.L. Pitt, and D.T. Spayde, Prog. in Part. Nucl. Phys. **54**, 289 (2005).
94. S.L. Zhu *et al.*, Phys. Rev. **D62**, 033008 (2000).
95. P. Souder, p. 599 of Ref. 5.
96. P. Langacker, p. 883 of Ref. 5.
97. R.D. Young *et al.*, Phys. Rev. Lett. **99**, 122003 (2007).
98. D.S. Armstrong and R.D. McKeown, Ann. Rev. Nucl. and Part. Sci. **62**, 337 (2012).
99. E. Derman and W.J. Marciano, Annals Phys. **121**, 147 (1979).
100. E158: P.L. Anthony *et al.*, Phys. Rev. Lett. **95**, 081601 (2005).
101. J. Erler and M.J. Ramsey-Musolf, Phys. Rev. **D72**, 073003 (2005).
102. J. Erler and R. Ferro-Hernández, JHEP **1803**, 196 (2018).

103. A. Czarnecki and W.J. Marciano, Int. J. Mod. Phys. A **15**, 2365 (2000).
104. C. Bouchiat and C.A. Piketty, Phys. Lett. **B128**, 73 (1983).
105. K.S. McFarland, in the *Proceedings of DIS* 2008.
106. Qweak: M.T. Gericke *et al.*, AIP Conf. Proc. **1149**, 237 (2009).
107. Qweak: R. Carlini *et al.*, `http://indico.ihep.ac.cn/event/6329/session/10/contribution/310/material/slides/0.pdf`.
108. For reviews and references to earlier work, see M.A. Bouchiat and L. Pottier, Science **234**, 1203 (1986);
B.P. Masterson and C.E. Wieman, p. 545 of Ref. 5.
109. M.S. Safronova *et al.*, `arXiv:1710.01833 [physics.atom-ph]`.
110. Cesium (Boulder): C.S. Wood *et al.*, Science **275**, 1759 (1997).
111. Cesium (Paris): J. Guéna, M. Lintz, and M.A. Bouchiat, Phys. Rev. **A71**, 042108 (2005).
112. Thallium (Oxford): N.H. Edwards *et al.*, Phys. Rev. Lett. **74**, 2654 (1995);
Thallium (Seattle): P.A. Vetter *et al.*, Phys. Rev. Lett. **74**, 2658 (1995).
113. Lead (Seattle): D.M. Meekhof *et al.*, Phys. Rev. Lett. **71**, 3442 (1993).
114. Bismuth (Oxford): M.J.D. MacPherson *et al.*, Phys. Rev. Lett. **67**, 2784 (1991).
115. P.G. Blunden, W. Melnitchouk and A.W. Thomas, Phys. Rev. Lett. **109**, 262301 (2012).
116. V.A. Dzuba, V.V. Flambaum, and O.P. Sushkov, Phys. Lett. **141A**, 147 (1989);
S.A. Blundell, J. Sapirstein, and W.R. Johnson, Phys. Rev. **D45**, 1602 (1992);
For reviews, see S.A. Blundell, W.R. Johnson, and J. Sapirstein, p. 577 of Ref. 5;
J.S.M. Ginges and V.V. Flambaum, Phys. Reports **397**, 63 (2004);
J. Guéna, M. Lintz, and M.A. Bouchiat, Mod. Phys. Lett. **A20**, 375 (2005);
A. Derevianko and S.G. Porsev, Eur. Phys. J. A **32**, 517 (2007).
117. V.A. Dzuba, V.V. Flambaum, and O.P. Sushkov, Phys. Rev. **A56**, R4357 (1997).
118. S.C. Bennett and C.E. Wieman, Phys. Rev. Lett. **82**, 2484 (1999).
119. M.A. Bouchiat and J. Guéna, J. Phys. (France) **49**, 2037 (1988).
120. S.G. Porsev, K. Beloy, and A. Derevianko, Phys. Rev. Lett. **102**, 181601 (2009).
121. V.A. Dzuba *et al.*, Phys. Rev. Lett. **109**, 203003 (2012);
B.M. Roberts, V.A. Dzuba and V.V. Flambaum, Ann. Rev. Nucl. and Part. Sci. **65**, 63 (2015).
122. A. Derevianko, Phys. Rev. Lett. **85**, 1618 (2000);
V.A. Dzuba, C. Harabati, and W.R. Johnson, Phys. Rev. **A63**, 044103 (2001);
M.G. Kozlov, S.G. Porsev, and I.I. Tupitsyn, Phys. Rev. Lett. **86**, 3260 (2001);
W.R. Johnson, I. Bednyakov, and G. Soff, Phys. Rev. Lett. **87**, 233001 (2001);
A.I. Milstein and O.P. Sushkov, Phys. Rev. **A66**, 022108 (2002);
V.A. Dzuba, V.V. Flambaum, and J.S. Ginges, Phys. Rev. **D66**, 076013 (2002);
M.Y. Kuchiev and V.V. Flambaum, Phys. Rev. Lett. **89**, 283002 (2002);
A.I. Milstein, O.P. Sushkov, and I.S. Terekhov, Phys. Rev. Lett. **89**, 283003 (2002);
V.V. Flambaum and J.S.M. Ginges, Phys. Rev. **A72**, 052115 (2005).
123. J. Erler, A. Kurylov, and M.J. Ramsey-Musolf, Phys. Rev. **D68**, 016006 (2003).
124. V.A. Dzuba *et al.*, J. Phys. **B20**, 3297 (1987).

125. Ya.B. Zel'dovich, Sov. Phys. JETP **6**, 1184 (1958);
V.V. Flambaum and D.W. Murray, Phys. Rev. **C56**, 1641 (1997);
W.C. Haxton and C.E. Wieman, Ann. Rev. Nucl. Part. Sci. **51**, 261 (2001).
126. J.L. Rosner, Phys. Rev. **D53**, 2724 (1996).
127. S.J. Pollock, E.N. Fortson, and L. Wilets, Phys. Rev. **C46**, 2587 (1992);
B.Q. Chen and P. Vogel, Phys. Rev. **C48**, 1392 (1993).
128. R.W. Dunford and R.J. Holt, J. Phys. **G34**, 2099 (2007).
129. O.O. Versolato *et al.*, Hyperfine Interact. **199**, 9 (2011).
130. W. Hollik and G. Duckeck, Springer Tracts Mod. Phys. **162**, 1 (2000).
131. D.Yu. Bardin *et al.*, `hep-ph/9709229`.
132. A. Czarnecki and J.H. Kühn, Phys. Rev. Lett. **77**, 3955 (1996);
R. Harlander, T. Seidensticker, and M. Steinhauser, Phys. Lett. **B426**, 125 (1998);
J. Fleischer *et al.*, Phys. Lett. **B459**, 625 (1999).
133. M. Awramik *et al.*, Nucl. Phys. **B813**, 174 (2009);
I. Dubovyk *et al.*, Phys. Lett. **B762**, 184 (2016).
134. A. Freitas, Phys. Lett. **B730**, 50 (2014) and JHEP **1404**, 070 (2014).
135. B.W. Lynn and R.G. Stuart, Nucl. Phys. **B253**, 216 (1985).
136. *Physics at LEP*, ed. J. Ellis and R. Peccei, CERN 86–02, Vol. 1.
137. PETRA: S.L. Wu, Phys. Reports **107**, 59 (1984);
C. Kiesling, *Tests of the Standard Theory of Electroweak Interactions*, (Springer-Verlag, New York, 1988);
R. Marshall, Z. Phys. **C43**, 607 (1989);
Y. Mori *et al.*, Phys. Lett. **B218**, 499 (1989);
D. Haidt, p. 203 of Ref. 5.
138. For reviews, see D. Schaile, p. 215, and A. Blondel, p. 277 of Ref. 5; P. Langacker [7]; and S. Riemann [139].
139. S. Riemann, Rept. on Prog. in Phys. **73**, 126201 (2010).
140. SLD: K. Abe *et al.*, Phys. Rev. Lett. **84**, 5945 (2000).
141. SLD: K. Abe *et al.*, Phys. Rev. Lett. **85**, 5059 (2000).
142. SLD: K. Abe *et al.*, Phys. Rev. Lett. **86**, 1162 (2001).
143. SLD: K. Abe *et al.*, Phys. Rev. Lett. **78**, 17 (1997).
144. P.A. Grassi, B.A. Kniehl, and A. Sirlin, Phys. Rev. Lett. **86**, 389 (2001).
145. CDF: T.A. Aaltonen *et al.*, Phys. Rev. **D93**, 112016 (2016).
146. DØ: V.M. Abazov *et al.*, `arXiv:1710.03951 [hep-ex]`.
147. CDF and DØ: T.A. Aaltonen *et al.*, `arXiv:1801.06283 [hep-ex]`.
148. DØ: V.M. Abazov *et al.*, Phys. Rev. **D84**, 012007 (2011).
149. CDF: D. Acosta *et al.*, Phys. Rev. **D71**, 052002 (2005).
150. H1: A. Aktas *et al.*, Phys. Lett. **B632**, 35 (2006).
151. ZEUS: H. Abramowicz *et al.*, Phys. Rev. **D93**, 092002 (2016).
152. ATLAS: G. Aad *et al.*, JHEP **1509**, 049 (2015).
153. CMS: `http://cds.cern.ch/record/2273392/files/SMP-16-007-pas.pdf`.
154. LHCb: R. Aaij *et al.*, JHEP **1511**, 190 (2015).
155. ALEPH, DELPHI, L3, OPAL, and LEP Electroweak Working Group: S. Schael *et al.*, Phys. Reports **532**, 119 (2013).

156. ALEPH, DELPHI, L3, OPAL, and LEP Electroweak Working Group: J. Alcaraz *et al.*, `hep-ex/0612034`.
157. A. Leike, T. Riemann, and J. Rose, Phys. Lett. **B273**, 513 (1991);
T. Riemann, Phys. Lett. **B293**, 451 (1992).
158. A comprehensive report and further references can be found in K.G. Chetyrkin, J.H. Kühn, and A. Kwiatkowski, Phys. Reports **277**, 189 (1996).
159. J. Schwinger, *Particles, Sources, and Fields*, Vol. II, (Addison-Wesley, New York, 1973);
K.G. Chetyrkin, A.L. Kataev, and F.V. Tkachev, Phys. Lett. **B85**, 277 (1979);
M. Dine and J. Sapirstein, Phys. Rev. Lett. **43**, 668 (1979);
W. Celmaster and R.J. Gonsalves, Phys. Rev. Lett. **44**, 560 (1980);
S.G. Gorishnii, A.L. Kataev, and S.A. Larin, Phys. Lett. **B259**, 144 (1991);
L.R. Surguladze, M.A. Samuel, Phys. Rev. Lett. **66**, 560 (1991) and *ibid.* 2416(E).
160. P.A. Baikov, K.G. Chetyrkin, and J.H. Kühn, Phys. Rev. Lett. **101**, 012002 (2008).
161. B.A. Kniehl and J.H. Kühn, Nucl. Phys. **B329**, 547 (1990);
K.G. Chetyrkin and A. Kwiatkowski, Phys. Lett. **B319**, 307 (1993);
S.A. Larin, T. van Ritbergen, and J.A.M. Vermaseren, Phys. Lett. **B320**, 159 (1994);
K.G. Chetyrkin and O.V. Tarasov, Phys. Lett. **B327**, 114 (1994).
162. A.L. Kataev, Phys. Lett. **B287**, 209 (1992).
163. D. Albert *et al.*, Nucl. Phys. **B166**, 460 (1980);
F. Jegerlehner, Z. Phys. **C32**, 425 (1986);
A. Djouadi, J.H. Kühn, and P.M. Zerwas, Z. Phys. **C46**, 411 (1990);
A. Borrelli *et al.*, Nucl. Phys. **B333**, 357 (1990).
164. A.A. Akhundov, D.Yu. Bardin, and T. Riemann, Nucl. Phys. **B276**, 1 (1986);
W. Beenakker and W. Hollik, Z. Phys. **C40**, 141 (1988);
B.W. Lynn and R.G. Stuart, Phys. Lett. **B352**, 676 (1990);
J. Bernabeu, A. Pich, and A. Santamaria, Phys. Lett. **B200**, 569 (1988) and Nucl. Phys. **B363**, 326 (1991).
165. H. Davoudiasl, H.-S. Lee, and W.J. Marciano, Phys. Rev. **D86**, 095009 (2012).
166. E. Braaten, S. Narison, and A. Pich, Nucl. Phys. **B373**, 581 (1992).
167. M. Davier *et al.*, Eur. Phys. J. **C74**, 2803 (2014).
168. F. Le Diberder and A. Pich, Phys. Lett. **B286**, 147 (1992).
169. M. Beneke and M. Jamin, JHEP **0809**, 044 (2008).
170. E. Braaten and C.S. Li, Phys. Rev. **D42**, 3888 (1990).
171. J. Erler, Rev. Mex. Fis. **50**, 200 (2004).
172. D. Boito *et al.*, Phys. Rev. **D85**, 093015 (2012).
173. D. Boito *et al.*, Phys. Rev. **D91**, 034003 (2015).
174. A. Pich, Prog. in Part. Nucl. Phys. **75**, 41 (2014);
A. Pich and A. Rodríguez-Sánchez, Phys. Rev. **D94**, 034027 (2016).
175. J. Erler, `arXiv:1102.5520 [hep-ph]`.
176. E821: G.W. Bennett *et al.*, Phys. Rev. Lett. **92**, 161802 (2004).

177. T. Aoyama *et al.*, Phys. Rev. Lett. **109**, 111808 (2012);
T. Aoyama *et al.*, PTEP **2012**, 01A107 (2012);
P. Baikov, A. Maier and P. Marquard, Nucl. Phys. **B877**, 647 (2013).
178. G. Li, R. Mendel, and M.A. Samuel, Phys. Rev. **D47**, 1723 (1993);
S. Laporta and E. Remiddi, Phys. Lett. **B301**, 440 (1993);
S. Laporta and E. Remiddi, Phys. Lett. **B379**, 283 (1996);
A. Czarnecki and M. Skrzypek, Phys. Lett. **B449**, 354 (1999).
179. J. Erler and M. Luo, Phys. Rev. Lett. **87**, 071804 (2001).
180. S. Laporta, Phys. Lett. **B772**, 232 (2017).
181. S.J. Brodsky and J.D. Sullivan, Phys. Rev. **D156**, 1644 (1967);
T. Burnett and M.J. Levine, Phys. Lett. **B24**, 467 (1967);
R. Jackiw and S. Weinberg, Phys. Rev. **D5**, 2473 (1972);
I. Bars and M. Yoshimura, Phys. Rev. **D6**, 374 (1972);
K. Fujikawa, B.W. Lee, and A.I. Sanda, Phys. Rev. **D6**, 2923 (1972);
G. Altarelli, N. Cabibbo, and L. Maiani, Phys. Lett. **B40**, 415 (1972);
W.A. Bardeen, R. Gastmans, and B.E. Laurup, Nucl. Phys. **B46**, 315 (1972).
182. T.V. Kukhto *et al.*, Nucl. Phys. **B371**, 567 (1992);
S. Peris, M. Perrottet, and E. de Rafael, Phys. Lett. **B355**, 523 (1995);
A. Czarnecki, B. Krause, and W.J. Marciano, Phys. Rev. **D52**, 2619 (1995);
A. Czarnecki, B. Krause, and W.J. Marciano, Phys. Rev. Lett. **76**, 3267 (1996);
C. Gnendiger, D. Stöckinger and H. Stöckinger-Kim, Phys. Rev. **D88**, 053005 (2013).
183. G. Degrassi and G. Giudice, Phys. Rev. **D58**, 053007 (1998);
A. Czarnecki, W.J. Marciano and A. Vainshtein, Phys. Rev. **D67**, 073006 (2003) and *ibid.* **D73**, 119901(E) (2006).
184. F. Jegerlehner *et al.*, EPJ Web Conf. **166**, 00022 (2018).
185. B. Chakraborty *et al.*, Phys. Rev. **D96**, 034516 (2017);
M. Della Morte *et al.*, JHEP **1710**, 020 (2017);
C. Lehner *et al.*, `arXiv:1710.06874 [hep-lat]`;
M. Della Morte *et al.*, `arXiv:1710.10072 [hep-lat]`;
S. Borsanyi *et al.*, `arXiv:1711.04980 [hep-lat]`;
T. Blum *et al.*, `arXiv:1801.07224 [hep-lat]`.
186. K. Melnikov and A. Vainshtein, Phys. Rev. **D70**, 113006 (2004).
187. J. Erler and G. Toledo Sánchez, Phys. Rev. Lett. **97**, 161801 (2006).
188. J. Prades, E. de Rafael, and A. Vainshtein, Adv. Ser. Direct. High Energy Phys. **20**, 303 (2009).
189. M. Knecht and A. Nyffeler, Phys. Rev. **D65**, 073034 (2002).
190. M. Hayakawa and T. Kinoshita, `hep-ph/0112102`;
J. Bijnens, E. Pallante, and J. Prades, Nucl. Phys. **B626**, 410 (2002);
A recent discussion is in J. Bijnens and J. Prades, Mod. Phys. Lett. **A22**, 767 (2007).
191. T. Blum *et al.*, Phys. Rev. Lett. **118**, 022005 (2017);
A. Gérardin *et al.*, `arXiv:1712.00421 [hep-lat]`.
192. B. Krause, Phys. Lett. **B390**, 392 (1997).

193. A. Kurz *et al.*, Phys. Lett. **B734**, 144 (2014);
A. Kurz *et al.*, EPJ Web Conf. **118**, 01033 (2016).
194. G. Colangelo *et al.*, Phys. Lett. **B735**, 90 (2014).
195. J.L. Lopez, D.V. Nanopoulos, and X. Wang, Phys. Rev. **D49**, 366 (1994).
196. U. Amaldi *et al.*, Phys. Rev. **D36**, 1385 (1987);
G. Costa *et al.*, Nucl. Phys. **B297**, 244 (1988);
P. Langacker and M. Luo, Phys. Rev. **D44**, 817 (1991);
J. Erler and P. Langacker, Phys. Rev. **D52**, 441 (1995).
197. CDF and DØ: T. Aaltonen *et al.*, Phys. Rev. **D88**, 052018 (2013).
198. ATLAS: M. Aaboud *et al.*, Eur. Phys. J. **C78**, 110 (2018).
199. Tevatron Electroweak Working Group, CDF and DØ: `arXiv:1003.2826 [hep-ex]`.
200. ATLAS and CMS: G. Aad *et al.*, Phys. Rev. Lett. **114**, 191803 (2015) and `http://cds.cern.ch/record/2052552/files/ATLAS-CONF-2015-044.pdf`.
201. ATLAS: `http://cds.cern.ch/record/2273853/files/ATLAS-CONF-2017-046.pdf`.
202. D. Sperka, in the *Proceedings of the 53rd Rencontres de Moriond – EW* 2018.
203. F. James and M. Roos, Comput. Phys. Commun. **10**, 343 (1975).
204. CMS: S. Chatrchyan *et al.*, Phys. Lett. **B728**, 496 (2014) and *ibid.* 526(E) (2014).
205. DØ: V.M. Abazov *et al.*, Phys. Rev. **D80**, 111107 (2009).
206. T. Klijnsma *et al.*, Eur. Phys. J. **C77**, 778 (2017).
207. P. Langacker and N. Polonsky, Phys. Rev. **D52**, 3081 (1995);
J. Bagger, K.T. Matchev, and D. Pierce, Phys. Lett. **B348**, 443 (1995).
208. M. Veltman, Nucl. Phys. **B123**, 89 (1977);
M. Chanowitz, M.A. Furman, and I. Hinchliffe, Phys. Lett. **B78**, 285 (1978);
The two-loop correction has been obtained by J.J. van der Bij and F. Hoogeveen, Nucl. Phys. **B283**, 477 (1987).
209. P. Langacker and M. Luo, Phys. Rev. **D45**, 278 (1992) and refs. therein.
210. A. Denner, R.J. Guth, and J.H. Kühn, Phys. Lett. **B240**, 438 (1990);
W. Grimus *et al.*, J. Phys. G **35**, 075001 (2008);
H.E. Haber and D. O'Neil, Phys. Rev. **D83**, 055017 (2011).
211. S. Bertolini and A. Sirlin, Phys. Lett. **B257**, 179 (1991).
212. M. Peskin and T. Takeuchi, Phys. Rev. Lett. **65**, 964 (1990);
M. Peskin and T. Takeuchi, Phys. Rev. **D46**, 381 (1992);
M. Golden and L. Randall, Nucl. Phys. **B361**, 3 (1991).
213. D. Kennedy and P. Langacker, Phys. Rev. **D44**, 1591 (1991).
214. G. Altarelli and R. Barbieri, Phys. Lett. **B253**, 161 (1991).
215. B. Holdom and J. Terning, Phys. Lett. **B247**, 88 (1990).
216. B.W. Lynn, M.E. Peskin, and R.G. Stuart, p. 90 of Ref. 136.
217. An alternative formulation is given by K. Hagiwara *et al.*, Z. Phys. **C64**, 559 (1994), and *ibid.* **68**, 352(E) (1995);
K. Hagiwara, D. Haidt, and S. Matsumoto, Eur. Phys. J. **C2**, 95 (1998).
218. I. Maksymyk, C.P. Burgess, and D. London, Phys. Rev. **D50**, 529 (1994);
C.P. Burgess *et al.*, Phys. Lett. **B326**, 276 (1994);
R. Barbieri, M. Frigeni, and F. Caravaglios, Phys. Lett. **B279**, 169 (1992).
219. R. Barbieri *et al.*, Nucl. Phys. **B703**, 127 (2004).

220. M.S. Carena *et al.*, Nucl. Phys. **B759**, 202 (2006).
221. R. Contino, `arXiv:1005.4269 [hep-ph]`.
222. E. Gates and J. Terning, Phys. Rev. Lett. **67**, 1840 (1991);
R. Sundrum and S.D.H. Hsu, Nucl. Phys. **B391**, 127 (1993);
R. Sundrum, Nucl. Phys. **B395**, 60 (1993);
M. Luty and R. Sundrum, Phys. Rev. Lett. **70**, 529 (1993);
T. Appelquist and J. Terning, Phys. Lett. **B315**, 139 (1993);
D.D. Dietrich, F. Sannino, and K. Tuominen, Phys. Rev. **D72**, 055001 (2005);
N.D. Christensen and R. Shrock, Phys. Lett. **B632**, 92 (2006);
M. Harada, M. Kurachi, and K. Yamawaki, Prog. Theor. Phys. **115**, 765 (2006).
223. H. Georgi, Nucl. Phys. **B363**, 301 (1991);
M.J. Dugan and L. Randall, Phys. Lett. **B264**, 154 (1991).
224. R. Barbieri *et al.*, Nucl. Phys. **B341**, 309 (1990).
225. J. Erler and D.M. Pierce, Nucl. Phys. **B526**, 53 (1998);
G.C. Cho and K. Hagiwara, Nucl. Phys. **B574**, 623 (2000);
G. Altarelli *et al.*, JHEP **0106**, 018 (2001);
S. Heinemeyer, W. Hollik, and G. Weiglein, Phys. Reports **425**, 265 (2006);
S.P. Martin, K. Tobe, and J.D. Wells, Phys. Rev. **D71**, 073014 (2005);
G. Marandella, C. Schappacher, and A. Strumia, Nucl. Phys. **B715**, 173 (2005);
M.J. Ramsey-Musolf and S. Su, Phys. Reports **456**, 1 (2008);
A. Djouadi, Phys. Reports **459**, 1 (2008);
S. Heinemeyer *et al.*, JHEP **0804**, 039 (2008);
O. Buchmueller *et al.*, Eur. Phys. J. **C72**, 2020 (2012).
226. B. Grinstein and M.B. Wise, Phys. Lett. **B265**, 326 (1991).
227. A. Pich, I. Rosell and J.J. Sanz-Cillero, JHEP **1401**, 157 (2014).
228. C.T. Hill and E.H. Simmons, Phys. Reports **381**, 235 (2003).
229. G. Panico and A. Wulzer, Lect. Notes Phys. **913**, 1 (2016).
230. J. Erler and P. Langacker, Phys. Rev. Lett. **105**, 031801 (2010).
231. CMS: S. Chatrchyan *et al.*, Phys. Rev. **D86**, 112003 (2012).
232. O. Eberhardt *et al.*, Phys. Rev. Lett. **109**, 241802 (2012);
A. Djouadi and A. Lenz, Phys. Lett. **B715**, 310 (2012).
233. J. Maalampi and M. Roos, Phys. Reports **186**, 53 (1990).
234. For reviews, see the Section on "Grand Unified Theories" in this *Review*;
P. Langacker, Phys. Reports **72**, 185 (1981);
J.L. Hewett and T.G. Rizzo, Phys. Reports **183**, 193 (1989);
J. Kang, P. Langacker and B.D. Nelson, Phys. Rev. **D77**, 035003 (2008);
S.P. Martin, Phys. Rev. **D81**, 035004 (2010);
P.W. Graham *et al.*, Phys. Rev. **D81**, 055016 (2010).
235. J. Erler, J.L. Feng, and N. Polonsky, Phys. Rev. Lett. **78**, 3063 (1997).
236. D. Choudhury, T.M.P. Tait, and C.E.M. Wagner, Phys. Rev. **D65**, 053002 (2002).
237. J. Erler and P. Langacker, Phys. Rev. Lett. **84**, 212 (2000).
238. P. Langacker and M. Plümacher, Phys. Rev. **D62**, 013006 (2000).
239. DELPHI: P. Abreu *et al.*, Eur. Phys. J. **C10**, 415 (1999).

240. P. Langacker and D. London, Phys. Rev. **D38**, 886 (1988);
D. London, p. 951 of Ref. 5;
a recent analysis is F. del Aguila, J. de Blas and M. Perez-Victoria, Phys. Rev. **D78**, 013010 (2008).
241. M. Chemtob, Prog. in Part. Nucl. Phys. **54**, 71 (2005);
R. Barbier *et al.*, Phys. Reports **420**, 1 (2005).
242. T. Han, H.E. Logan, and L.T. Wang, JHEP **0601**, 099 (2006);
M. Perelstein, Prog. in Part. Nucl. Phys. **58**, 247 (2007).
243. K. Agashe *et al.*, JHEP **0308**, 050 (2003);
M. Carena *et al.*, Phys. Rev. **D68**, 035010 (2003);
I. Gogoladze and C. Macesanu, Phys. Rev. **D74**, 093012 (2006);
I. Antoniadis, `hep-th/0102202`;
see also the note on "Extra Dimensions" in the Searches Particle Listings.
244. A. Pomarol and F. Riva, JHEP **1401**, 151 (2014);
J. Ellis, V. Sanz and T. You, JHEP **1503**, 157 (2015);
A. Efrati, A. Falkowski and Y. Soreq, JHEP **1507**, 018 (2015);
J. de Blas *et al.*, `arXiv:1710.05402 [hep-ph]`.
245. G. Altarelli, R. Barbieri, and S. Jadach, Nucl. Phys. **B369**, 3 (1992) and *ibid.* **B376**, 444(E) (1992).
246. G.C. Cho, K. Hagiwara, and S. Matsumoto, Eur. Phys. J. **C5**, 155 (1998);
K. Cheung, Phys. Lett. **B517**, 167 (2001);
Z. Han and W. Skiba, Phys. Rev. **D71**, 075009 (2005).
247. P. Langacker, M. Luo, and A.K. Mann, Rev. Mod. Phys. **64**, 87 (1992);
M. Luo, p. 977 of Ref. 5.
248. F.S. Merritt *et al.*, p. 19 of *Particle Physics: Perspectives and Opportunities: Report of the DPF Committee on Long Term Planning*, ed. R. Peccei *et al.* (World Scientific, Singapore, 1995).